Cell Reports

Article

Regulatory T Cells Play a Role in a Subset of Idiopathic Preterm Labor/Birth and Adverse Neonatal Outcomes

Graphical Abstract

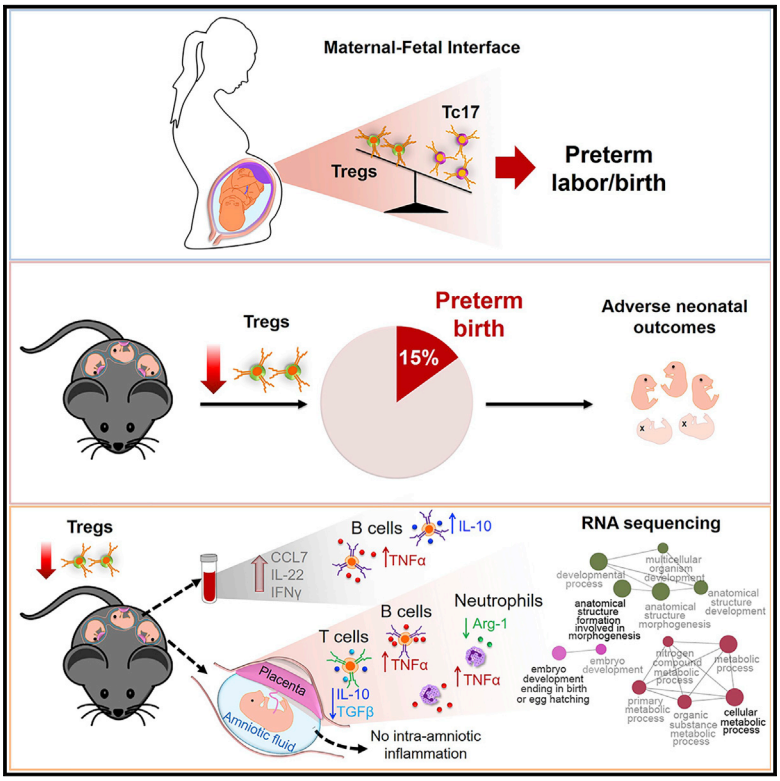

Highlights

- Tregs are reduced at the maternal-fetal interface in idiopathic preterm labor/birth
- The loss of Tregs induces a fraction of preterm births
- The loss of Tregs induces adverse fetal and neonatal outcomes
- Tregs modulate systemic and local immune responses in the third period of pregnancy

Authors

Nardhy Gomez-Lopez, Marcia Arenas-Hernandez, Roberto Romero, ..., Carmen Sanchez-Torres, Bogdan Done, Adi L. Tarca

Correspondence

nardhy.gomez-lopez@wayne.edu

In Brief

Understanding of the role of regulatory T cells in late gestation has been limited. Gomez-Lopez et al. provide evidence that Tregs modulate immune responses in the third period of pregnancy. Treg deficiency contributes to a subset of formerly idiopathic preterm births and adverse perinatal outcomes.

Gomez-Lopez et al., 2020, Cell Reports *32*, 107874
July 7, 2020
https://doi.org/10.1016/j.celrep.2020.107874

CellPress

Cell Reports

CellPress
OPEN ACCESS

Article

Regulatory T Cells Play a Role in a Subset of Idiopathic Preterm Labor/Birth and Adverse Neonatal Outcomes

Nardhy Gomez-Lopez,[1,2,3,12,*] Marcia Arenas-Hernandez,[1,2,4] Roberto Romero,[1,5,6,7,8,9] Derek Miller,[1,2] Valeria Garcia-Flores,[1,2] Yaozhu Leng,[1,2] Yi Xu,[1,2] Jose Galaz,[1,2] Sonia S. Hassan,[1,2,10] Chaur-Dong Hsu,[1,2,10] Harley Tse,[3] Carmen Sanchez-Torres,[4] Bogdan Done,[1,2] and Adi L. Tarca[1,2,11]

[1]Perinatology Research Branch, Division of Obstetrics and Maternal-Fetal Medicine, Division of Intramural Research, *Eunice Kennedy Shriver* National Institute of Child Health and Human Development, National Institutes of Health, U.S. Department of Health and Human Services, Detroit, MI 48201, USA

[2]Department of Obstetrics and Gynecology, Wayne State University School of Medicine, Detroit, MI 48201, USA

[3]Department of Immunology, Microbiology and Biochemistry, Wayne State University School of Medicine, Detroit, MI 48201, USA

[4]Departamento de Biomedicina Molecular, Centro de Investigacion y de Estudios Avanzados del Instituto Politecnico Nacional, Mexico City 07360, Mexico

[5]Department of Obstetrics and Gynecology, University of Michigan, Ann Arbor, MI 48109, USA

[6]Department of Epidemiology and Biostatistics, Michigan State University, East Lansing, MI 48824, USA

[7]Center for Molecular Medicine and Genetics, Wayne State University, Detroit, MI 48201, USA

[8]Detroit Medical Center, Detroit, MI 48201, USA

[9]Department of Obstetrics and Gynecology, Florida International University, Miami, FL 33199, USA

[10]Department of Physiology, Wayne State University School of Medicine, Detroit, MI 48201, USA

[11]Department of Computer Science, Wayne State University College of Engineering, Detroit, MI 48201, USA

[12]Lead Contact

*Correspondence: nardhy.gomez-lopez@wayne.edu

https://doi.org/10.1016/j.celrep.2020.107874

SUMMARY

Regulatory T cells (Tregs) have been exhaustively investigated during early pregnancy; however, their role later in gestation is poorly understood. Herein, we report that functional Tregs are reduced at the maternal-fetal interface in a subset of women with idiopathic preterm labor/birth, which is accompanied by a concomitant increase in Tc17 cells. In mice, depletion of functional Tregs during late gestation induces preterm birth and adverse neonatal outcomes, which are rescued by the adoptive transfer of such cells. Treg depletion does not alter obstetrical parameters in the mother, yet it increases susceptibility to endotoxin-induced preterm birth. The mechanisms whereby depletion of Tregs induces adverse perinatal outcomes involve tissue-specific immune responses and mild systemic maternal inflammation, together with dysregulation of developmental and cellular processes in the placenta, in the absence of intra-amniotic inflammation. These findings provide mechanistic evidence supporting a role for Tregs in the pathophysiology of idiopathic preterm labor/birth and adverse neonatal outcomes.

INTRODUCTION

Preterm birth is a leading cause of perinatal morbidity and mortality worldwide (Blencowe et al., 2012; Liu et al., 2015). Preterm neonates are at high risk for multiple short- and long-term complications, accounting for more than two million neonatal deaths in 2010 and representing an enormous burden for society and the health care system (Howson et al., 2013). Preterm birth is preceded by spontaneous preterm labor (PTL), a syndrome of multiple putative etiologies (Romero et al., 2014a). Among these, only acute pathological inflammation (i.e., intra-amniotic infection/inflammation and clinical chorioamnionitis) has been well characterized and causally linked to preterm labor (Romero et al., 1988; Gravett et al., 1994; Combs et al., 2014; Oh et al., 2017; Deng et al., 2019). The remaining etiologies are poorly understood; therefore, most cases of preterm birth (approximately 60%) are characterized as idiopathic (Goldenberg et al., 2008; Barros et al., 2015). A breakdown of maternal-fetal tolerance has been suggested as a mechanism of disease for idiopathic preterm labor and birth (Romero et al., 2014a; Gomez-Lopez et al., 2014). However, to date, no causal evidence has been provided connecting impaired maternal-fetal tolerance with preterm labor/birth and its adverse perinatal outcomes.

Maternal-fetal tolerance is established locally (e.g., the maternal-fetal interface) and systemically by the mother toward the allogeneic conceptus (Chaouat et al., 1979; Bonney and Onyekwuluje, 2003; Aluvihare et al., 2004; Zenclussen et al., 2005; Robertson et al., 2009; Kahn and Baltimore, 2010; Shima

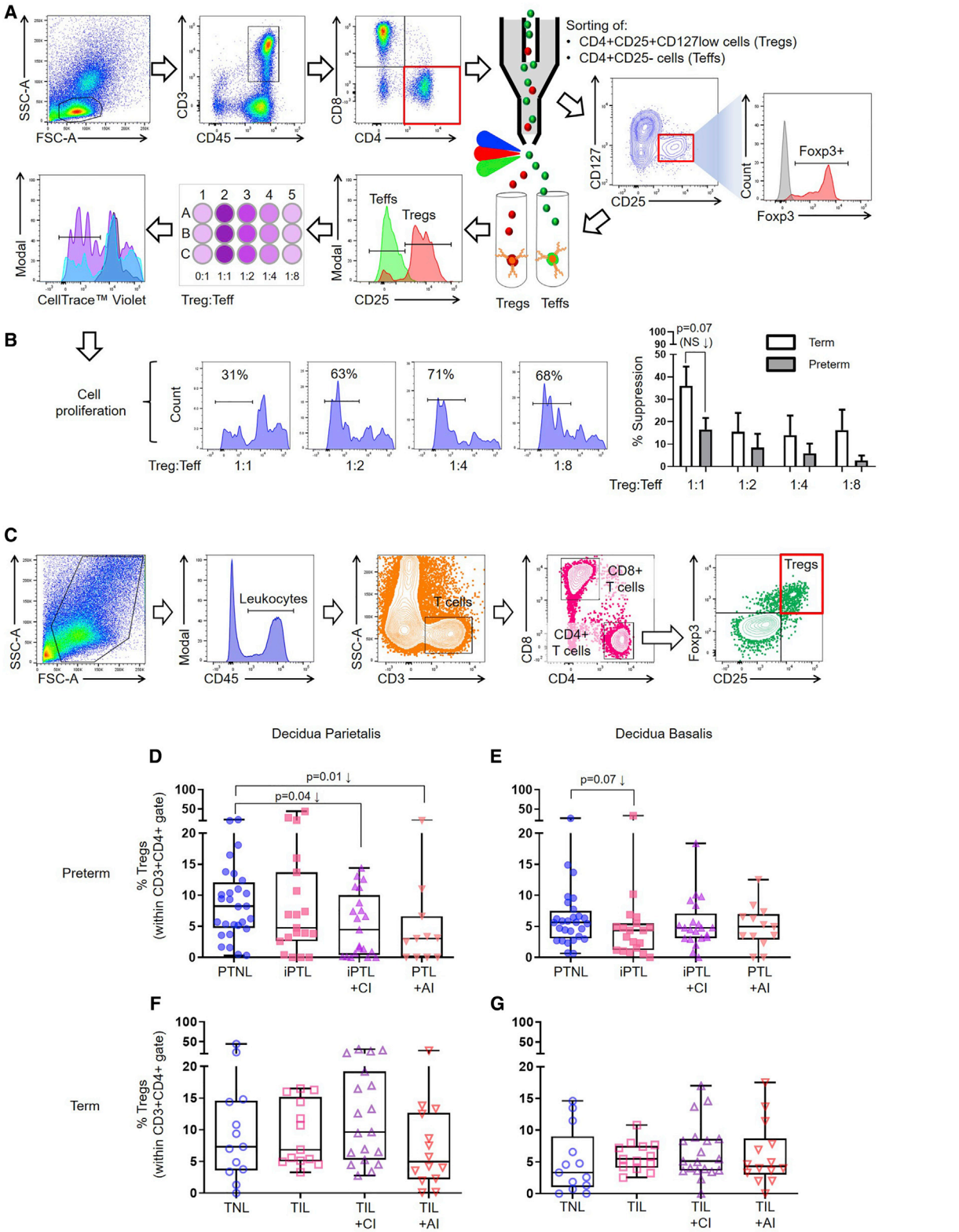

Figure 1. Functional Tregs Are Reduced at the Human Maternal-Fetal Interface in a Subset of Idiopathic PTL and birth

(A) Representative gating strategy used to sort Tregs and Teffs from the decidua. Tregs were co-cultured with Teffs, and Teff proliferation was measured by flow cytometry using CellTrace violet.

(legend continued on next page)

et al., 2010, 2015; Samstein et al., 2012; Rowe et al., 2012). At the maternal-fetal interface, this tolerance is sustained by an immune repertoire composed of regulatory T cells (Tregs) (Aluvihare et al., 2004; Sasaki et al., 2004; Heikkinen et al., 2004; Tsuda et al., 2018; Salvany-Celades et al., 2019), as well as homeostatic innate immune cells such as macrophages (Hunt et al., 1984; Gustafsson et al., 2008; Houser et al., 2011; Svensson et al., 2011; Svensson-Arvelund et al., 2015; Xu et al., 2016), natural killer (NK) cells (Kieckbusch et al., 2015; Li et al., 2017), and innate lymphoid cells (Vacca et al., 2015; Doisne et al., 2015; Xu et al., 2018; Miller et al., 2018). To date, most research has focused on investigating the processes of maternal-fetal tolerance during early pregnancy (Zenclussen et al., 2005; Kahn and Baltimore, 2010; Shima et al., 2010; Samstein et al., 2012; Rowe et al., 2012; Chen et al., 2013), given that this is the period in which the growing conceptus educates the maternal immune system to sustain pregnancy and promote its survival (Arck and Hecher, 2013; Robertson et al., 2018; Tsuda et al., 2019). However, the role of Tregs later in gestation (third trimester in humans and third week in mice) has not been mechanistically investigated.

Clinical studies have shown a negative association between the numbers and/or function of peripheral Tregs and the diagnosis of PTL leading to preterm birth (Xiong et al., 2010; Schober et al., 2012; Steinborn et al., 2012; Gomez-Lopez and Laresgoiti-Servitje, 2012). However, whether Tregs are reduced in number and/or function at the maternal-fetal interface (i.e., decidua) in women with PTL is unknown. Herein, we undertook an extensive investigation that included both human decidual samples from different subsets of PTL and animal models, which allowed us to provide translational and mechanistic evidence of a role for Tregs in the pathophysiology of idiopathic preterm labor/birth and adverse neonatal outcomes.

RESULTS

Functional Tregs Are Reduced at the Maternal-Fetal Interface in a Subset of Women with Idiopathic PTL and birth

The maternal-fetal interface represents the site of immune interactions between the mother and the conceptus (Chaouat et al., 1983; Petroff, 2005; Erlebacher, 2013; PrabhuDas et al., 2015; Bonney, 2016). The human maternal-fetal interface includes (1) the decidua parietalis, the area of contact between the endometrium and the chorioamniotic membranes, and (2) the decidua basalis, the interface between the endometrium and the placenta (Sindram-Trujillo et al., 2003; Gomez-Lopez et al., 2013). Different subsets of Tregs have been localized in both the decidua basalis (Sindram-Trujillo et al., 2004; Sasaki et al., 2004; Tilburgs et al., 2006, 2008; Inada et al., 2013; Tsuda et al., 2018; Salvany-Celades et al., 2019) and the decidua parietalis (Sindram-Trujillo et al., 2004; Heikkinen et al., 2004; Tilburgs et al., 2006, 2008; Salvany-Celades et al., 2019); however, their suppressive activity has yet to be established. We first tested whether third-trimester-derived decidual Tregs had suppressive activity. Decidual Tregs were sorted from preterm and term decidual tissues (Table S1) and co-cultured with matched isolated effector T cells (Teffs) (Figure 1A), and the percentage of suppression was calculated (see STAR Methods). Decidual Tregs exhibited suppressive activity at a 1:1 Treg:Teff ratio, yet such a function seemed to be lower in preterm pregnancies compared to term pregnancies (Figure 1B). These data show that third-trimester decidual Tregs display suppressive activity toward Teffs at the human maternal-fetal interface.

Next, we investigated whether Tregs were altered at the maternal-fetal interface of women who underwent the pathological (preterm) or physiological (term) process of labor. To address this research question, we collected decidual tissues from women with PTL and birth or term labor/birth (TIL), as well as gestational age-matched non-labor controls (preterm without labor [PTNL] or term without labor [TNL]) (Table S2). Given that the process of labor can occur in the setting of acute inflammation of the placenta (Kim et al., 2015a), resulting from intra-amniotic inflammation/infection, the well-known etiology of preterm birth (Romero et al., 1989), we subdivided the preterm and term labor groups according to the presence or absence of acute chorioamnionitis (AI) (Table S2). Idiopathic PTL (iPTL) was subdivided by the presence (iPTL+CI) or absence (iPTL) of chronic chorioamnionitis (CI) (Kim et al., 2015b), a placental lesion associated with maternal anti-fetal rejection (Lee et al., 2011). Neither of the iPTL groups included the presence of acute inflammation of the placental tissues. Leukocytes were isolated from the decidua basalis and decidua parietalis based on our previously established method (Xu et al., 2015), and flow cytometry was used to determine the frequencies of Tregs (CD45+CD3+CD4+CD25+Foxp3+ cells) (Figure 1C). In the decidua parietalis, Tregs were significantly reduced in women with iPTL+CI compared to non-labor controls (Figure 1D). A slight non-significant reduction in Tregs was also observed in women with iPTL compared to non-labor controls (Figure 1D). Moreover, in the decidua basalis, Tregs tended to be reduced in women with iPTL (Figure 1E). Decidual Tregs were also reduced in women whose placentas displayed acute inflammatory lesions (Figure 1D), as previously shown in the uterine tissues of mice injected with an endotoxin (animal model of acute systemic inflammation-induced preterm birth)

(B) Representative plots showing the proliferation of Teffs, with the percentage of decidual Treg suppression of Teffs from preterm and term pregnancies. Suppression data are shown as means ± SEM. n = 6–8 per group.

(C) Representative gating strategy used to identify Tregs in the decidua parietalis and decidua basalis.

(D and E) Frequency of Tregs in the (D) decidua parietalis (n = 11–28 per group) or (E) decidua basalis (n = 13–28 per group) of women with PTNL, iPTL, iPTL+CI, or PTL+AI.

(F and G) Frequency of Tregs in the (F) decidua parietalis (n = 13–19 per group) or (G) decidua basalis (n = 13–19 per group) of women with TNL, TIL, TIL+CI, or TIL+AI.

Data are represented as medians with interquartile and minimum/maximum ranges. Statistical analysis was performed using the Mann-Whitney U-test. Demographic and clinical characteristics of the study population are shown in Tables S1 and S2.

(Arenas-Hernandez et al., 2016). No differences were observed among the term groups (Figures 1F and 1G). These findings show that Tregs are reduced at the maternal-fetal interface in a subset of women who underwent the pathological process of idiopathic PTL and birth, but not in those who underwent the physiological process of labor at term.

Tc17 Cells Are Increased at the Maternal-Fetal Interface in Women with Idiopathic PTL and birth

It has been proposed that a balance exists during normal pregnancy between homeostatic Tregs and pro-inflammatory Th17 cells, and a breakdown of this balance leads to obstetrical disease (Saito et al., 2010; Figueiredo and Schumacher, 2016). Therefore, we investigated whether the reduction in decidual Tregs in women with PTL and birth was accompanied by a concomitant increase in decidual Th17 cells. Flow cytometry was performed to determine the frequencies of Th17 cells (CD45+CD3+CD4+IL-17A+ cells) (Figure 2A) in the decidua (Table S2). Neither the decidua parietalis nor the decidua basalis displayed significant changes in the frequencies of Th17 cells among the preterm and term study groups (Figures 2B–2E). Given that interleukin (IL)-17A is also produced by CD8+ T cells, Tc17 cells (CD45+CD3+CD8+IL-17A+ cells), and that such cells display a pro-inflammatory phenotype (Hamada et al., 2009; Huber et al., 2009), these cells were identified in the decidua (Figure 2A). Consistently, both in the decidua parietalis and decidua basalis, the frequencies of Tc17 cells were greater in women with iPTL compared to non-labor controls (Figures 2F and 2G). Again, no differences were observed in the frequencies of Tc17 cells among the term study groups (Figures 2H and 2I). These findings show that an imbalance between functional Tregs and Tc17 cells occurs at the maternal-fetal interface in women with idiopathic PTL and birth.

Establishment of a Model to Study the Role of Systemic Tregs in Late Pregnancy

Together with clinical studies (Xiong et al., 2010; Schober et al., 2012; Steinborn et al., 2012; Gomez-Lopez and Laresgoiti-Servitje, 2012), our first set of data (Figure 1) indicates that women with PTL and birth have reduced Tregs both in the peripheral circulation and at the maternal-fetal interface. Next, we undertook *in vivo* experimentation to demonstrate a causal link between systemic Tregs and preterm birth.

Previous studies showed that the systemic depletion of Tregs before implantation or in early gestation results in failure to implant or pregnancy loss (Zenclussen et al., 2005; Darrasse-Jèze et al., 2006; Kahn and Baltimore, 2010; Shima et al., 2010; Rowe et al., 2011, 2012; Samstein et al., 2012; Chen et al., 2013). However, to date, no studies have established a role for systemic Tregs in the third week of murine pregnancy (i.e., third trimester in humans). An earlier study depleted allogeneic CD25+ T cells on 10.5 and 13.5 days postcoitum (dpc), and no adverse pregnancy outcomes were recorded (Shima et al., 2010). A possible explanation as to why the depletion of CD25+ T cells did not cause disease in the previously mentioned study is that the depletion of CD25+ T cells is incomplete and not specific for Foxp3+ Tregs (Kohm et al., 2006; Couper et al., 2007; Fan et al., 2018). Alternatively, it could be that Tregs were not functional during the third week of murine pregnancy, as they were in earlier pregnancy (Polanczyk et al., 2005). Therefore, we first determined whether murine Tregs displayed suppressive activity in the second and third weeks of pregnancy (Figure S1A). As expected, second-week-derived Tregs suppressed Teff proliferation (Figure S1B). Third-week-derived Tregs also suppressed Teff proliferation (Figure S1C). Indeed, at a 1:8 Treg:Teff ratio, third-week-derived Tregs were more suppressive than second-week-derived Tregs (Figure S1D). Thus, Tregs are functional during the second and third weeks of murine pregnancy.

We then proceeded to establish a murine model in which the partial or total depletion of Tregs can be achieved in the third week of pregnancy. We reasoned that the partial depletion of Tregs will resemble the clinical condition in which women have reduced Tregs (e.g., PTL) (Figure 1), whereas the total depletion of Tregs will allow us to definitively establish a role for such cells in pregnancy. We used *Foxp3*^{DTR} mice (Kim et al., 2007), in which the administration of diphtheria toxin (DT) allows for depletion of all Foxp3+ Tregs. The administration of 25 μg/kg (Rowe et al., 2011, 2012) or 50 μg/kg (Kim et al., 2007; Samstein et al., 2012) of DT to naive non-pregnant *Foxp3*^{DTR} mice induced the partial or total depletion of Tregs, respectively, as indicated by the reduction of these cells in the uterine-draining lymph nodes (ULNs), spleen, and thymus (Figure S2). Next, we mated *Foxp3*^{DTR} females with BALB/c males to obtain an allogeneic pregnancy (Figure 3A; Figure S3A). To induce the partial or total depletion of Tregs, *Foxp3*^{DTR} dams were injected with 25 or 50 μg/kg of DT on 14.5 dpc, followed by daily administration of 5 or 50 μg/kg of DT, respectively, until delivery (Figure 3A; Figure S3A). The partial or total depletion of Tregs was confirmed in the decidua, myometrium, peripheral blood, and placenta (Figure 3B), as well as the ULNs, inguinal lymph nodes, mesenteric lymph nodes, spleen, and thymus (Figures S3B–S3F). These experiments established the murine models to study the role of Tregs in the third week of pregnancy (i.e., third trimester in humans, when the onset of preterm labor occurs).

Systemic Depletion of Tregs Induces a Fraction of Preterm Births and Causes Adverse Neonatal Outcomes in the First Pregnancy

During the first pregnancy, the partial or total depletion of Tregs in the third week induced a 15% or 10% rate of preterm birth, respectively (Figure 3C). In addition, neonates born to partially or totally Treg-depleted *Foxp3*^{DTR} dams displayed increased mortality from birth to three weeks of age (Figure 3D). However, no differences were observed between those born to partially and those born to totally Treg-depleted *Foxp3*^{DTR} dams (Figure 3D). Moreover, surviving neonates born to partially or totally Treg-depleted *Foxp3*^{DTR} dams were leaner than those from controls at one, two, and three weeks postpartum (Figures 3E–3G), but this effect was more drastic in neonates born to totally Treg-depleted *Foxp3*^{DTR} dams (Figures 3F–3G). Given the adverse effects of the depletion of Tregs on neonatal outcomes, we also investigated whether the partial or total depletion of Tregs affected fetal growth *in utero*. Representative images of the fetuses and placentas from control (PBS), partially

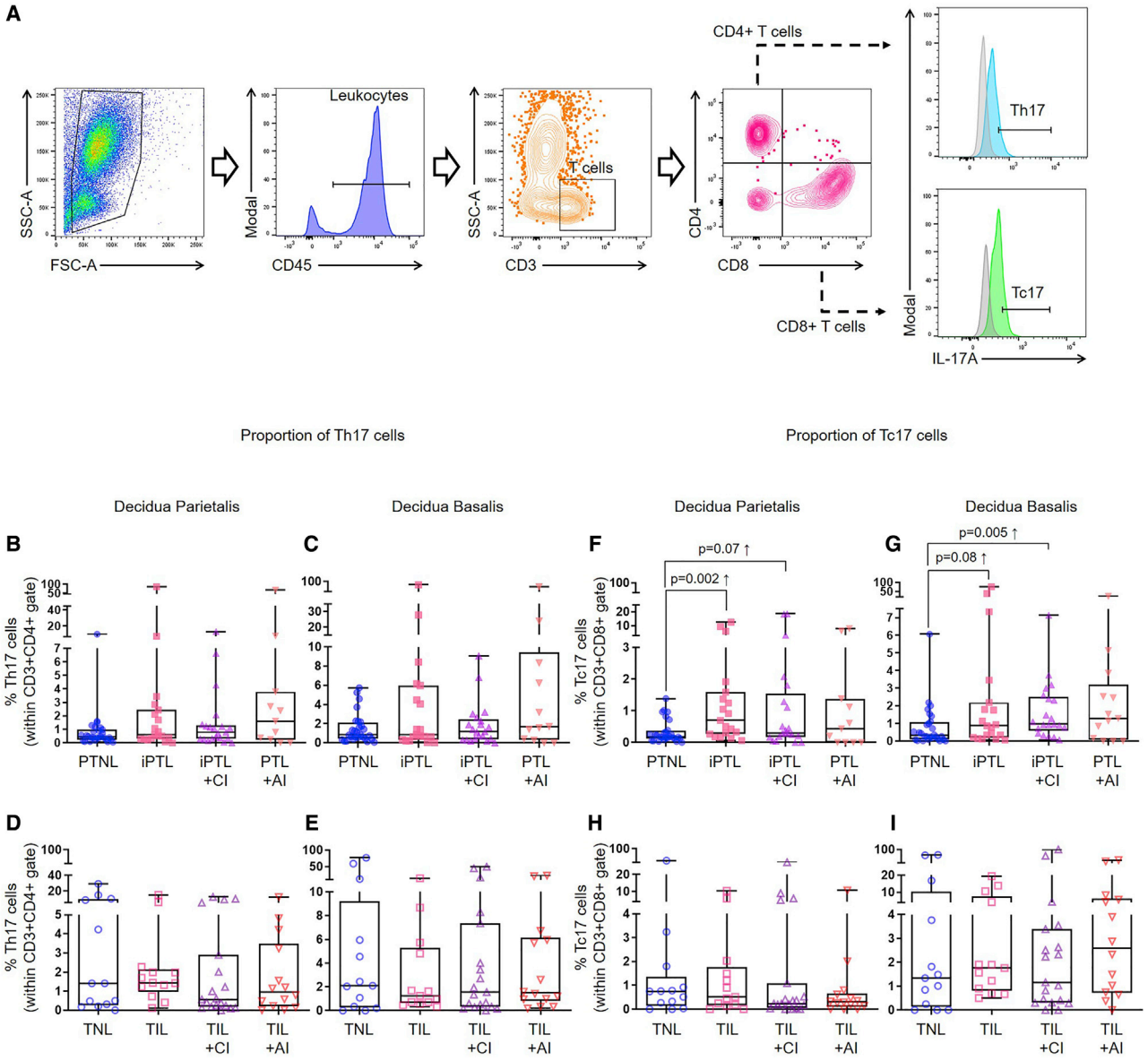

Figure 2. Tc17 Cells Are Increased at the Human Maternal-Fetal Interface in Idiopathic PTL and birth

(A) Representative gating strategy used to identify Th17 cells and Tc17 cells in the decidua parietalis and decidua basalis.

(B and C) Frequency of Th17 cells in the (B) decidua parietalis (n = 11–28 per group) or (C) decidua basalis (n = 13–28 per group) of women with PTNL, iPTL, iPTL+CI, or PTL+AI.

(D and E) Frequency of Th17 cells in the (D) decidua parietalis (n = 13–19 per group) or (E) decidua basalis (n = 13–19 per group) of women with TNL, TIL, TIL+CI, or TIL+AI.

(F and G) Frequency of Tc17 cells in the (F) decidua parietalis (n = 11–28 per group) or (G) decidua basalis (n = 13–28 per group) of women with PTNL, iPTL, iPTL+CI, or PTL+AI.

(H and I) Frequency of Tc17 cells in the (H) decidua parietalis (n = 13–19 per group) or (I) decidua basalis (n = 13–19 per group) of women with TNL, TIL, TIL+CI, or TIL+AI.

Data are represented as medians with interquartile and minimum/maximum ranges. Statistical analysis was performed using the Mann-Whitney U-test. Demographic and clinical characteristics of the study population are shown in Table S2.

Treg-depleted, or totally Treg-depleted *Foxp3*^{DTR} dams are shown in Figure 3H. Fetuses from partially and totally Treg-depleted *Foxp3*^{DTR} dams were smaller and leaner than those from controls (Figures 3H and 3I), indicating that the depletion of Tregs affects fetal growth. However, placental weights were similar between controls and Treg-depleted mice (Figure 3J). These results show that the partial or total depletion of Tregs in the third week of the first pregnancy induces a fraction of preterm birth and, importantly, adverse fetal and neonatal outcomes.

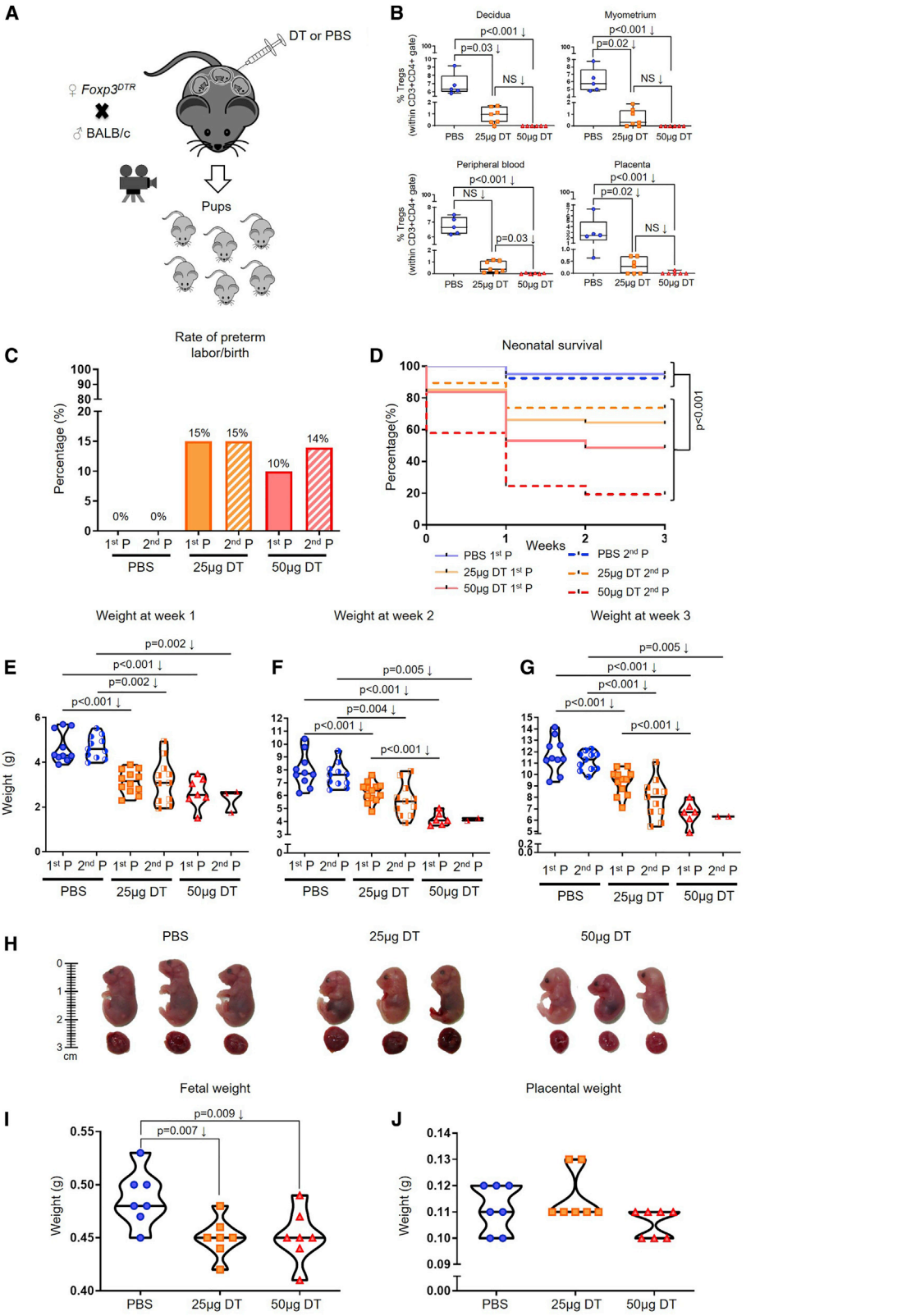

(legend on next page)

Systemic Depletion of Tregs Induces a Fraction of Preterm Births and Causes Adverse Neonatal Outcomes in Repeat Pregnancies

A prior study has shown that Tregs undergo an accelerated expansion during the second pregnancy, which confers resilience against pregnancy loss (Rowe et al., 2012). Therefore, we reasoned that the total depletion of Tregs during the first and second pregnancy will worsen the rate of preterm birth and/or adverse neonatal outcomes observed during the first pregnancy. To examine this research question, Tregs were partially or totally depleted during the first and second pregnancy. The repeated partial or total depletion of Tregs induced comparable rates of preterm birth to the first pregnancy (15% and 14%, respectively) (Figure 3C). As observed in the first pregnancy, neonates born to partially and totally Treg-depleted *Foxp3*^{DTR} dams during repeat pregnancies had higher rates of mortality compared to controls (Figure 3D). The repeated total depletion of Tregs in the first and second pregnancy induced a greater rate of neonatal mortality than the partial depletion of Tregs, a phenomenon that was not observed during the first pregnancy (Figure 3D). Like the first pregnancy, surviving neonates from partially or totally Treg-depleted *Foxp3*^{DTR} dams during repeat pregnancies were leaner than their control counterparts at weeks one, two, and three postpartum (Figures 3E–3G). These results show that the repeated partial or total depletion of Tregs in the first and second pregnancy results in rates of preterm birth that are comparable to those of the first pregnancy. Nonetheless, the total depletion of Tregs in the first and second pregnancy had more deleterious effects on neonatal survival than the depletion of such cells in the first pregnancy alone.

The Adoptive Transfer of Tregs Prevents Preterm Birth and Adverse Neonatal Outcomes

Next, we evaluated whether the adoptive transfer of Tregs could prevent the adverse pregnancy outcomes induced by the depletion of such cells. Tregs were isolated from allogeneic pregnancies and adoptively transferred to partially Treg-depleted *Foxp3*^{DTR} dams on 14.5 and 16.5 dpc, and pregnancy outcomes were recorded (Figure 4A). The rate of preterm birth in partially Treg-depleted *Foxp3*^{DTR} dams was rescued by the adoptive transfer of Tregs (15% versus 0%) (Figure 4B). Moreover, neonatal survival at one, two, and three weeks of age was significantly improved after the adoptive transfer of Tregs (Figure 4C). The proportion of adoptively transferred Tregs was also determined using EGFP-expressing mice (see STAR Methods and Key Resources Table) (Figure 4D). Adoptively transferred Tregs were observed in the peripheral blood, ULNs, spleen, decidua, myometrium, and placenta (Figure 4E). These results provide a mechanistic demonstration that Tregs play a role in the timing of parturition and neonatal survival.

Systemic Depletion of Tregs Increases the Susceptibility to Endotoxin-Induced Preterm Birth

The depletion of Tregs did not always induce preterm birth (Figure 3C). Therefore, we reasoned that the loss of such cells, in some cases, could increase the susceptibility to lipopolysaccharide (LPS or endotoxin)-induced preterm birth. Partially Treg-depleted *Foxp3*^{DTR} dams received a mild dose of LPS (that does not cause preterm birth in wild-type mice) on 16.5 dpc and were monitored until delivery (Figure S4A). The injection of LPS in Treg-depleted *Foxp3*^{DTR} dams induced a 33% rate of preterm birth, whereas all non-Treg-depleted *Foxp3*^{DTR} dams delivered at term (Figure S4B). Moreover, the injection of LPS caused a higher rate of neonatal mortality in Treg-depleted *Foxp3*^{DTR} dams than in non-Treg-depleted *Foxp3*^{DTR} dams (Figure S4C). *Foxp3*^{DTR} dams injected with DT alone (on 14.5 and 15.5 dpc) did not deliver preterm, and their neonates thrived for up to 3 weeks, as controls did (data not shown). These findings indicate that the depletion of Tregs also increases the susceptibility of the mother to deliver preterm upon encountering inflammatory agents (e.g., bacterial infection).

Systemic Depletion of Tregs Does Not Negatively Affect Maternal Obstetrical Parameters

Previous studies have shown that the long-term depletion of Tregs induces systemic disease (Kim et al., 2007; Gousopoulos et al., 2016), including severe acute inflammation (Kim et al., 2007). This finding raised the question as to whether the total or partial depletion of Tregs used in the current study could

Figure 3. Depletion of Tregs Induces a Fraction of Preterm Births and Adverse Neonatal Outcomes

(A) *Foxp3*^{DTR} dams underwent partial or total Treg depletion. Controls were injected with sterile 1× PBS. After the first pregnancy (P), a subset of *Foxp3*^{DTR} dams underwent a second P and were again partially or totally Treg-depleted or were injected with sterile 1× PBS.

(B) Frequencies of Tregs in the decidua, myometrium, peripheral blood, and placenta of partially or totally Treg-depleted *Foxp3*^{DTR} dams (n = 5–7 per group). Data are represented as medians with interquartile and minimum/maximum ranges.

(C) Preterm birth rates of non-Treg-depleted-, partially Treg-depleted-, and totally Treg-depleted-*Foxp3*^{DTR} dams (1st or 2nd P, n = 9–20 per group). Data are represented as means of percentages.

(D) Percentage of survival from birth until 3 weeks postpartum for neonates born to non-Treg-depleted-, partially Treg-depleted-, and totally Treg-depleted-*Foxp3*^{DTR} dams (1st or 2nd P, n = 7–18 per group).

(E–G) Weights of neonates born to non-Treg-depleted-, partially Treg-depleted-, and totally Treg-depleted-*Foxp3*^{DTR} dams at weeks (E) 1, (F) 2, and (G) 3 postpartum (1st or 2nd P, n = 2–12 litters per group). Data are represented as violin plots with medians and minimum/maximum ranges.

(H) Representative images of fetuses (and their placentas) from non-Treg-depleted-, partially Treg-depleted-, and totally Treg-depleted-*Foxp3*^{DTR} dams (n = 8–9 per group).

(I and J) Weights of (I) fetuses and (J) their placentas from non-Treg-depleted-, partially Treg-depleted-, and totally Treg-depleted-*Foxp3*^{DTR} dams (n = 7 litters per group).

Statistical analysis was performed using the Mantel-Cox test for survival curves, and Kruskal-Wallis or ANOVA tests with correction for multiple comparisons. See also Figures S1–S4.

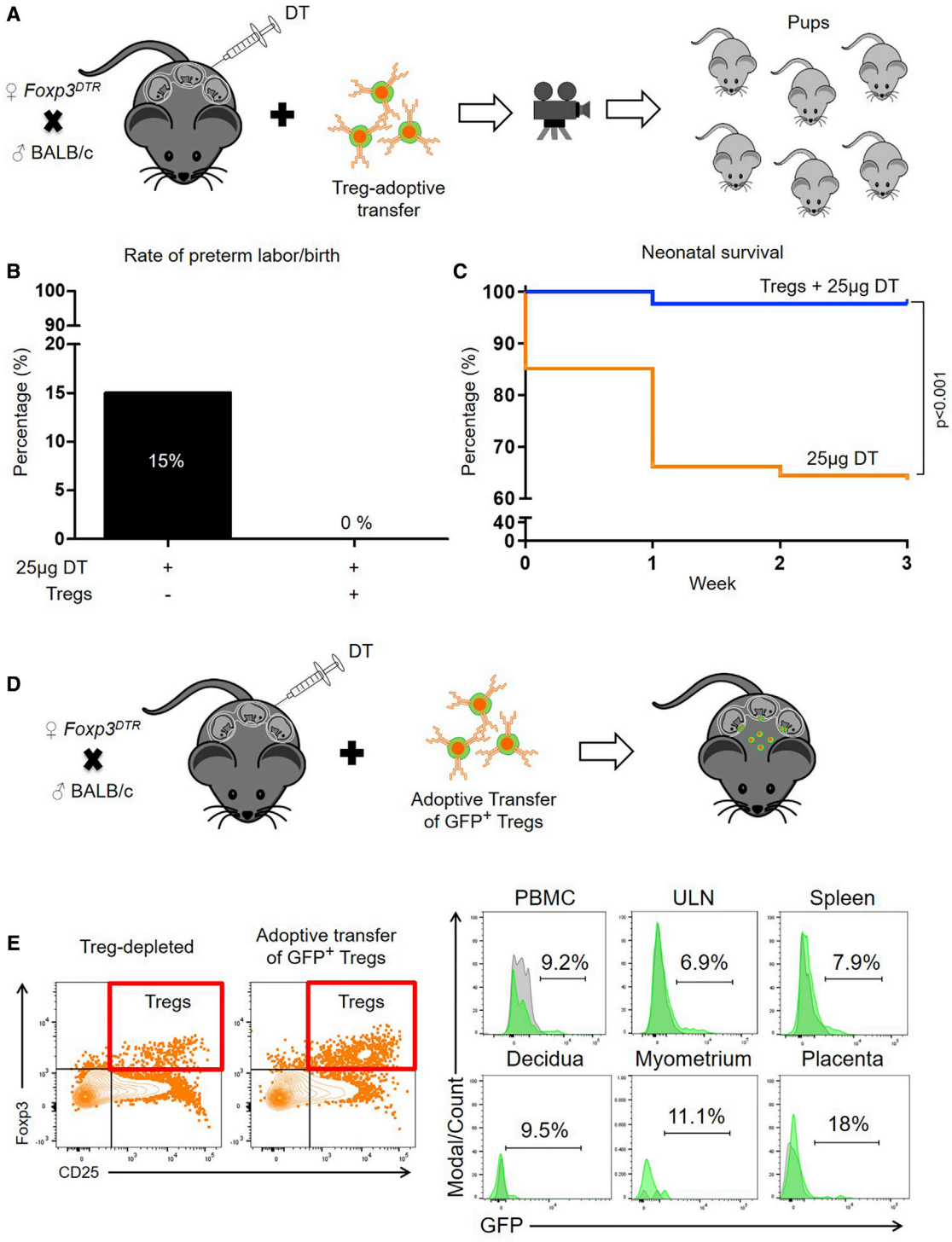

Figure 4. The Adoptive Transfer of Tregs Prevents Preterm Birth and Adverse Neonatal Outcomes

(A) *Foxp3*^{DTR} dams underwent partial Treg depletion. On 14.5 and 16.5 dpc, *Foxp3*^{DTR} dams received an adoptive transfer of Tregs from wild-type mice.

(B) Preterm birth rates of partially Treg-depleted *Foxp3*^{DTR} dams without or with the adoptive transfer of Tregs (n = 6–20 per group). Data are represented as means of percentages.

(C) Percentage of survival from birth until 3 weeks postpartum for neonates born to partially Treg-depleted *Foxp3*^{DTR} dams without or with the adoptive transfer of Tregs (n = 6–20 per group).

(legend continued on next page)

cause systemic acute disease that, in turn, may be the cause of mice delivering preterm. We argue that this could not be the case because the Treg depletion used herein was solely performed during the third week of pregnancy. Nonetheless, we conducted a series of obstetrical determinations that are commonly performed in pregnant women to evaluate maternal and fetal well-being (Sotiriadis et al., 2019; Poon et al., 2019). Partially and totally Treg-depleted *Foxp3*^{DTR} dams, as well as control dams, underwent body temperature monitoring, blood pressure determination, and high-resolution ultrasound imaging (Figure 5A) (see STAR Methods). Systemic acute inflammation induces hypothermia in mice (Gomez-Lopez et al., 2018); however, the depletion of Tregs did not cause hypothermia. Thus, partially and totally Treg-depleted *Foxp3*^{DTR} dams displayed body temperature similar to that of control dams (Figure 5B). In addition, partially and totally Treg-depleted *Foxp3*^{DTR} dams had blood pressure similar to that of control dams (Figure 5C). Uterine artery Doppler allowed the determination of the maternal heart rate and uterine artery pulsatility index (Figure 5D). Partially and totally Treg-depleted *Foxp3*^{DTR} dams had heart rates similar to those of control dams (Figure 5E). Totally Treg-depleted *Foxp3*^{DTR} dams had reduced uterine artery pulsatility indices compared to control dams (Figure 5F). However, only an increased uterine artery Doppler is associated with hypertensive disorders (e.g., preeclampsia) and adverse perinatal outcomes (Poon et al., 2019). Umbilical artery Doppler allowed the determination of the fetal heart rate and umbilical artery pulsatility index (Figure 5G). Fetuses of totally, but not partially, Treg-depleted *Foxp3*^{DTR} dams were bradycardic (reduced heart rates compared to controls) (Figure 5H), which is consistent with our earlier observations showing that Treg depletion causes fetal compromise (Figures 3H and 3I). However, fetuses of partially and totally Treg-depleted *Foxp3*^{DTR} dams displayed umbilical artery pulsatility indices similar to those of control fetuses (Figure 5I). The latter finding is relevant, because an abnormal umbilical artery pulsatility index is associated with a cytokine storm in the maternal circulation (Gomez-Lopez et al., 2016a), indicating that Treg depletion is not associated with severe acute inflammation in the maternal circulation.

The long-term depletion of Tregs causes splenomegaly (Kim et al., 2007); therefore, we also evaluated the size of the spleens and ULNs. Partially and totally Treg-depleted *Foxp3*^{DTR} dams had a similar-sized spleen compared to control dams, but ULNs of totally Treg-depleted dams were slightly enlarged (Figure 5J). However, neonates of partially or totally Treg-depleted *Foxp3*^{DTR} dams that survived were breastfed by the dams (Figure 5K; see milk band indicating that newborns were breastfed).

These physiological determinations show that the depletion of Tregs during the third week of pregnancy neither negatively affects maternal obstetrical parameters nor induces splenomegaly or alters breastfeeding, yet it induces fetal compromise.

Systemic Depletion of Tregs Induces a Mild Inflammatory Response in the Maternal Circulation that Can Induce Early-Term Delivery

Next, we investigated whether the depletion of Tregs alters cytokine responses in the maternal circulation. This question arose from some cases of preterm labor being characterized by diverse inflammatory responses in the maternal circulation (Gervasi et al., 2001; Sorokin et al., 2010; Cruciani et al., 2010; Cobo et al., 2013; Park et al., 2018). However, these systemic immune responses vary between subsets of preterm labor; therefore, the determination of specific cytokines in the maternal circulation is not useful to predict preterm birth. Regardless, we reasoned that by using targeted approaches (e.g., Treg depletion), we may be able to observe stereotypical immune responses in the maternal circulation that may otherwise be difficult to identify in humans. *Foxp3*^{DTR} dams underwent partial or total depletion of Tregs, and in preterm gestations, the maternal plasma was collected for determination of 36 cytokines using a multiplex system (see STAR Methods and Key Resources Table). Consistent with our hypothesis, the depletion of Tregs did not increase the conventional acute pro-inflammatory cytokines IL-6, CCL2, IL-1β, and tumor necrosis factor alpha (TNF-α) in the maternal circulation (Figures 6A–6D). As expected (Garcia-Flores et al., 2018), these and other acute pro-inflammatory cytokines were increased in a model of endotoxin-induced preterm birth, but not in the partially or totally Treg-depleted *Foxp3*^{DTR} dams (Figure S5). Interestingly, totally Treg-depleted *Foxp3*^{DTR} dams displayed higher plasma concentrations of interferon gamma (IFNγ), CCL7, and IL-22 compared to control dams (Figures 6E–6G). The plasma concentrations of IL-10 (a cytokine produced by Tregs) (Kemper et al., 2003) tended to be reduced in Treg-depleted *Foxp3*^{DTR} dams; however, this reduction did not reach statistical significance (Figure 6H). To complement these observations, we tested whether systemic administration of IFNγ, CCL7, and IL-22 at pathological concentrations (concentrations found in the maternal circulation upon Treg depletion) could induce preterm birth and neonatal mortality (see STAR Methods and Key Resources Table), as Treg depletion does. Systemic administration of CCL7 and IL-22, but not IFNγ, shortened the gestational length but was insufficient to induce preterm birth (i.e., delivery before 18.5 dpc) (Figure 6I). Thus, a fraction of dams injected with CCL7 and/or IL-22 underwent early-term delivery (Figure 6J). However, pups born to dams injected with CCL7 and/or IL-22 did not show significantly higher mortality rates at birth compared to controls (Figure 6K). The combined administration of CCL7 and IL-22 resulted in similar outcomes to those observed with the single administration of each cytokine (data not shown). Collectively, these results indicate that the mild inflammatory response observed in Treg-depleted dams partially participates in the timing of parturition but alone is not sufficient to induce preterm birth or neonatal mortality.

(D) *Foxp3*^{DTR} dams underwent partial Treg depletion. On 14.5 and 16.5 dpc, *Foxp3*^{DTR} dams received an adoptive transfer of Tregs from *EGFP* mice.
(E) Representative gating and histograms showing adoptively transferred GFP+ Tregs in the decidua, myometrium, placenta, and peripheral tissues (peripheral blood mononuclear cells [PBMCs], uterine-draining lymph nodes [ULNs], and spleen) of recipient Treg-depleted dams. Statistical analysis was performed using the Mantel-Cox test for survival curves.

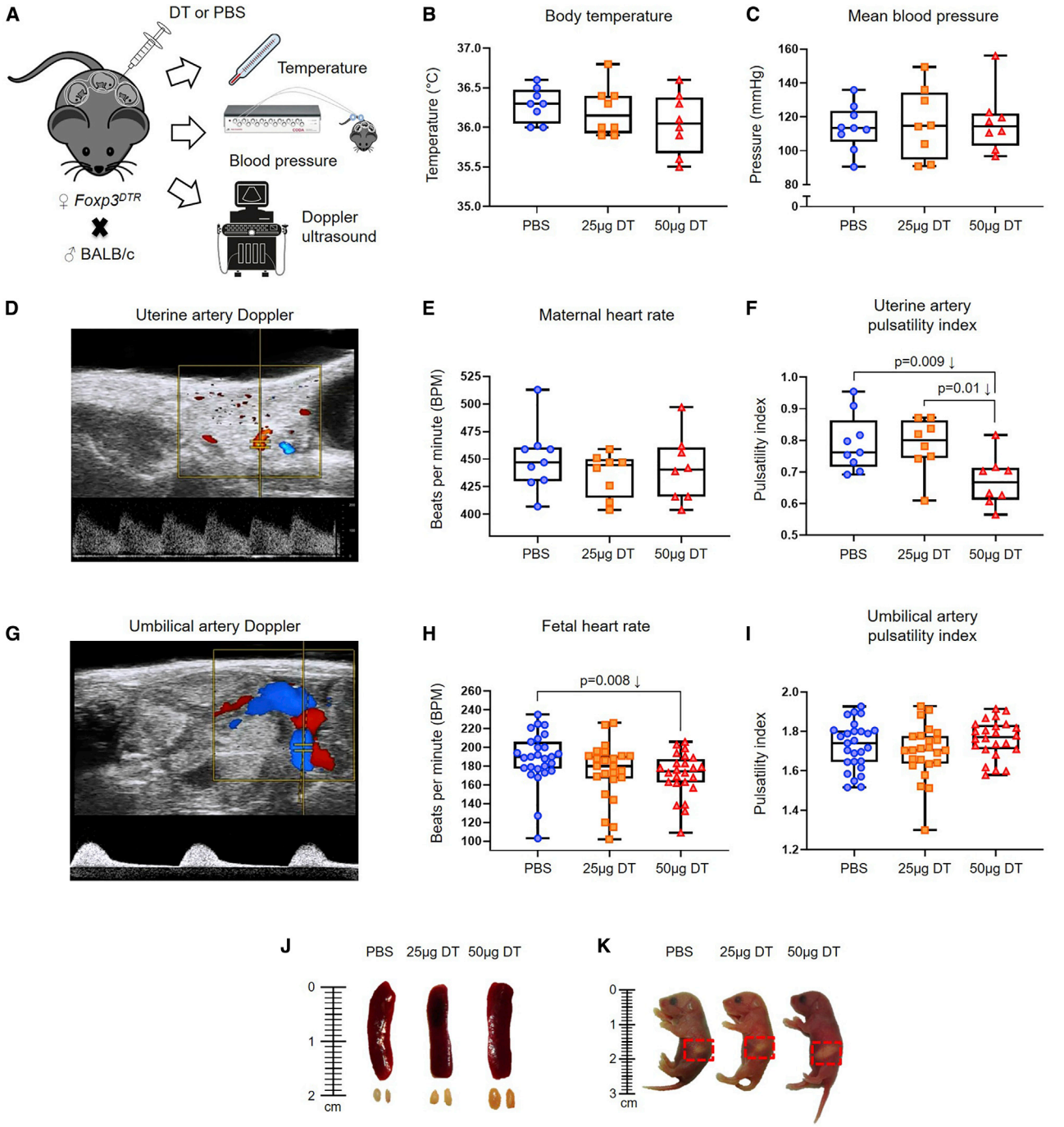

Figure 5. Maternal-Fetal Obstetrical Parameters upon Partial or Total Treg Depletion

(A) *Foxp3*^{DTR} dams underwent partial or total Treg depletion until 17.5 dpc on which body temperature, blood pressure, and Doppler determinations were performed (n = 8–9 per group).

(B and C) Body temperature (B) and mean blood pressure (C) of non-Treg-depleted-, partially Treg-depleted-, and totally Treg-depleted-*Foxp3*^{DTR} dams (n = 8–9 per group).

(D–F) Representative Doppler image of the uterine artery (D), which was used to determine (E) maternal heart rate, and (F) uterine artery pulsatility index of non-Treg-depleted-, partially Treg-depleted-, and totally Treg-depleted-*Foxp3*^{DTR} dams (n = 8–9 per group).

(legend continued on next page)

Systemic Depletion of Tregs Does Not Cause Intra-amniotic Inflammation

Until this point, we have shown that the depletion of Tregs causes fetal compromise and adverse neonatal outcomes in the absence of a severe acute inflammatory response in the maternal circulation. This scenario resembles the subclinical presentation of PTL (Barros et al., 2015). However, some of these cases occur in the presence of localized sterile intra-amniotic inflammation (Romero et al., 2015). Therefore, we next explored whether the partial or total depletion of Tregs affects the cytokine network in the amniotic cavity. *Foxp3*^{DTR} dams underwent partial or total depletion of Tregs, and in preterm gestations, amniotic fluid was collected to determine 36 cytokines by using a multiplex system (see STAR Methods and Key Resources Table). The depletion of Tregs did not induce an intra-amniotic inflammatory response (Figures 6L–6S). Indeed, pro-inflammatory cytokines—IL-6 (Yoon et al., 2001; Gervasi et al., 2012; Combs et al., 2014; Romero et al., 2014b, 2014c), CXCL10 (Kim et al., 2010; Romero et al., 2017), CCL2 (Esplin et al., 2005), and others (Romero et al., 1992, 2015; Cox et al., 1997; Dudley et al., 1997)—that have been reported to be elevated in some cases of intra-amniotic inflammation/infection-associated preterm labor were unchanged in Treg-depleted dams compared to controls (Figures 6L–6Q). Stereotypical anti-inflammatory cytokines, namely, IL-10 (D'Andrea et al., 1993; de Waal Malefyt et al., 1993; Wei et al., 2017) and IL-4 (Hart et al., 1989; Fenton et al., 1992), were also unchanged upon the depletion of such cells (Figures 6R and 6S). These results show that the reduction of Tregs can lead to adverse perinatal outcomes in the absence of an intra-amniotic inflammatory response, resembling idiopathic PTL.

Systemic Depletion of Tregs Induces Specific Cellular Immune Responses at the Maternal-Fetal Interface, in the Placenta, and in the Maternal Circulation

To further explore the mechanisms whereby the loss of Tregs induces adverse perinatal outcomes, we explored the cellular repertoire at the maternal-fetal interface, in the placenta, and in the maternal circulation. This research question was based on previous studies showing that PTL involves stereotypical cellular responses at the maternal-fetal interface (Arenas-Hernandez et al., 2016, 2019; St Louis et al., 2016; Xu et al., 2016; Gomez-Lopez et al., 2017a; Rinaldi et al., 2017; Garcia-Flores et al., 2018; Xu et al., 2018; Leng et al., 2019; Slutsky et al., 2019), in the placenta (Salafia et al., 1991; Redline and Patterson, 1994; Kim et al., 2009, 2015b; Gill et al., 2019), and in the maternal circulation (Gervasi et al., 2001; Pique-Regi et al., 2019). *Foxp3*^{DTR} dams underwent partial or total depletion of Tregs, and the decidua, myometrium, placenta, and peripheral blood were collected in preterm gestations. Immunophenotyping was performed, and data were represented in heatmaps (see STAR Methods). Overall, the partial or total depletion of Tregs in *Foxp3*^{DTR} dams induced specific immune alterations in the cellular repertoire among compartments (Figure 7A; Figure S6). Specifically, the partial depletion of Tregs in *Foxp3*^{DTR} dams reduced Arg1+ B cells and increased total macrophages in the decidual tissues (Figure 7A). In the myometrium, the total depletion of Tregs consistently reduced transforming growth factor β (TGF-β)+ and IL-10+ CD4+ T cells (Figure S6), as well as Arg1+ neutrophils (Figure 7A). In the maternal circulation, the depletion of Tregs caused the reduction of inducible nitric oxide synthase (iNOS)+ dendritic cells and an increase in TNF-α+ B cells (Figure 7A). Similar to the maternal circulation, Treg depletion induced cellular responses in the placental tissues; however, these changes did not hold statistical significance after adjustment for multiple comparisons (Figure 7A). Altogether, these data show that Tregs modulate the expression of specific mediators by immune cells present at the maternal-fetal interface, in the placenta, and in the maternal circulation.

RNA-Seq Analysis Reveals that Tregs Are Central for Regulation of Developmental and Cellular Processes in the Placenta

The loss of Tregs induces fetal growth restriction (Figures 3H and 3I), whose pathophysiology involves placental disease (Burton and Jauniaux, 2018). Therefore, we next used RNA sequencing (RNA-seq) to survey the molecular processes dysregulated in the placenta upon Treg depletion (see STAR Methods). The partial depletion of Tregs caused mild dysregulation of the placental transcriptome (Figures 7B and 7C; Tables S3 and S4). However, the total depletion of Tregs caused significant dysregulation of several physiological processes in the placenta (Figures 7B and 7D). Specifically, total depletion of Tregs induced the upregulation of 568 genes and the downregulation of 286 genes (Figure 7D; Tables S5 and S6). The dysregulated pathways included embryo development ending in birth, anatomical structure formation involved in morphogenesis, cellular macromolecule localization, cellular metabolic process, cellular component biogenesis, and actin cytoskeleton organization (Figure 7E; Tables S7 and S8). This last set of data demonstrates that Tregs play a role in fetal life and provides a possible explanation as to why the offspring of Treg-depleted dams display impaired growth and, more importantly, adverse neonatal outcomes.

DISCUSSION

This study provides descriptive and mechanistic evidence showing a role for Tregs in the pathophysiology of a subset of idiopathic preterm labors/births and adverse neonatal outcomes. First, we showed that functional Tregs are reduced at the human maternal-fetal interface in a subset of women with

(G–I) Representative Doppler image of the umbilical artery (G), which was used to determine (H) fetal heart rate, and (I) umbilical artery pulsatility index in fetuses of non-Treg-depleted-, partially Treg-depleted-, and totally Treg-depleted-*Foxp3*^{DTR} dams (n = 24–27 per group).

(J) Representative images of the spleens and ULNs from non-Treg-depleted-, partially Treg-depleted-, and totally Treg-depleted-*Foxp3*^{DTR} dams (n = 3 per group).

(K) Representative images of neonates born to non-Treg-depleted-, partially Treg-depleted-, and totally Treg-depleted-*Foxp3*^{DTR} dams on the day of birth (n = 3 per group). Red dotted squares indicate the presence of the milk band. Statistical analysis was performed using the Kruskal-Wallis or ANOVA tests with correction for multiple comparisons.

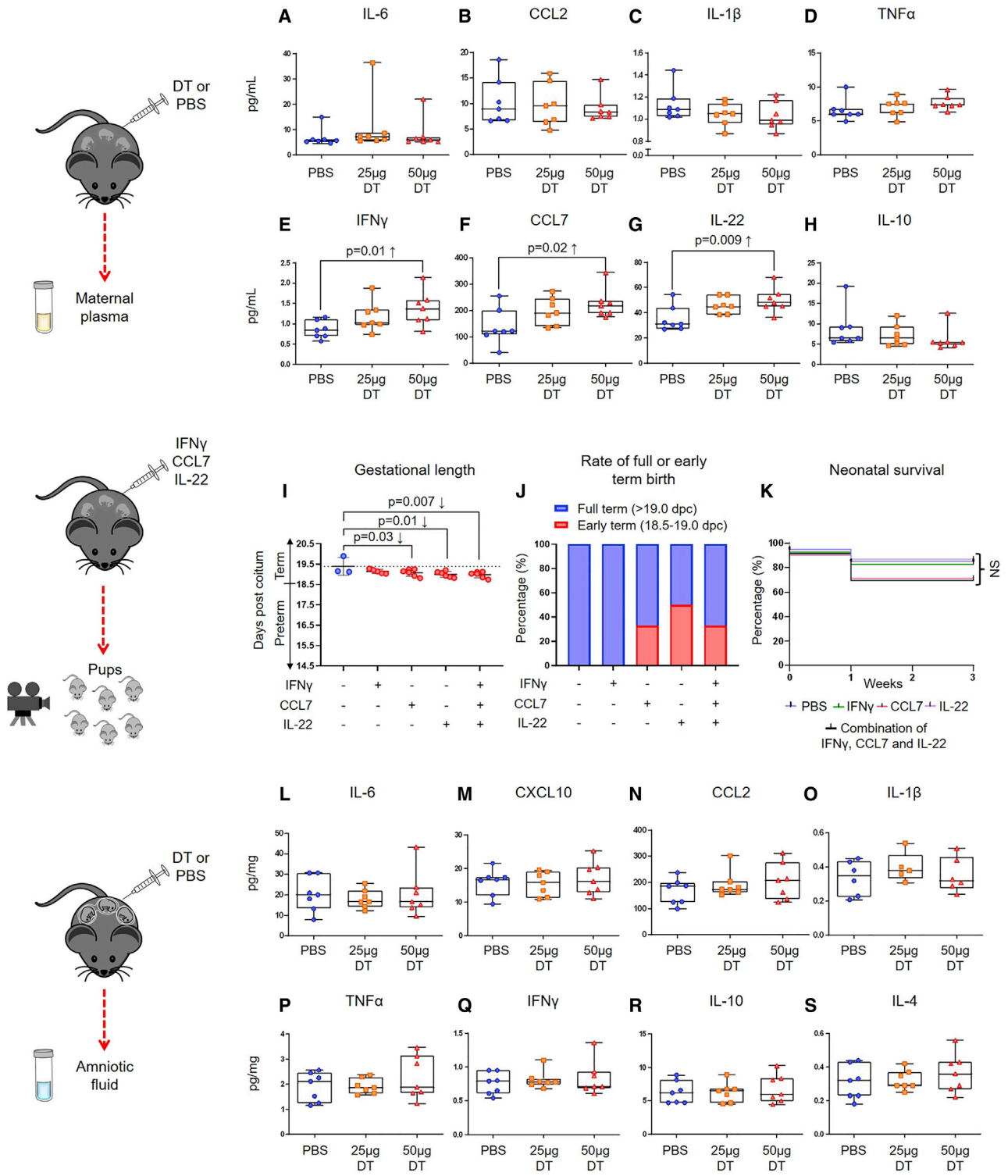

Figure 6. Depletion of Tregs Induces a Mild Systemic Inflammatory Response in the Absence of Intra-Amniotic Inflammation

(A–H) *Foxp3*^{DTR} dams underwent partial or total Treg depletion. Controls were injected with sterile 1× PBS. Mice were euthanized approximately 4 h after the second DT or PBS injection, and maternal plasma samples and amniotic fluid were collected. Concentrations of (A) IL-6, (B) CCL2, (C) IL-1β, (D) TNF-α, (E) IFNγ, (F) CCL7, (G) IL-22, and (H) IL-10 in the maternal plasma (n = 7 per group). Data are shown as medians with interquartile ranges and minimum/maximum ranges. C57BL/6 dams were intravenously injected with recombinant mouse IFNγ (1.4 pg/100 μL), CCL7 (218 pg/100 μL), IL-22 (48 pg/100 μL), or a combination of all three. Controls were injected with 100 μL of sterile 1× PBS alone.

(legend continued on next page)

idiopathic PTL and birth. This finding is consistent with previous clinical reports showing that women with PTL display a reduction in the suppressive activity of peripheral Tregs (Schober et al., 2012; Gomez-Lopez and Laresgoiti-Servitje, 2012). Therefore, both peripheral and local Tregs are reduced in women who undergo spontaneous PTL and birth. However, the reduction in Tregs at the maternal-fetal interface does not occur in the physiological process of labor at term. This latter finding is in line with the hypothesis that some cases of preterm labor are mediated through a mechanism different from term parturition (Holt et al., 2011; Gomez-Lopez et al., 2017b; Yellon, 2017; Willcockson et al., 2018; Paquette et al., 2018; Pereyra et al., 2019). The most marked reduction of Tregs occurred at the area of contact between the endometrium and the fetal chorioamniotic membranes (i.e., decidua parietalis) in the presence of chronic inflammation of the placenta, which is a pathological process mediated by effector activated T cells (Kim et al., 2015b; Arenas-Hernandez et al., 2019). These data allowed us to hypothesize that the decline in Tregs in the decidua parietalis is accompanied by augmented T-cell responses at the maternal-fetal interface in a subset of women who underwent idiopathic PTL and birth.

Effector memory CD4+ and CD8+ T cells are present at the human maternal-fetal interface in term and preterm gestations (van der Zwan et al., 2018; Arenas-Hernandez et al., 2019; Slutsky et al., 2019). These T cells are increased in women with preterm labor, leading to preterm birth (Arenas-Hernandez et al., 2019). In the current study, we provide further data indicating that decidual CD8+ T cells expressing IL-17A are implicated in the pathophysiology of preterm parturition in the absence of acute inflammation in the placenta (i.e., idiopathic preterm birth). In addition to the inflammatory cytokine IL-17A (Yao et al., 1995; Fossiez et al., 1996; Onishi and Gaffen, 2010; McGeachy et al., 2019), most Tc17 cells secrete pro-inflammatory mediators such as TNF-α and IL-2 but have reduced cytotoxic activity (Hamada et al., 2009; Huber et al., 2009); therefore, we suggest that the imbalance between Tregs and Tc17 cells at the human maternal-fetal interface creates a hostile inflammatory milieu that leads to preterm parturition, even in the absence of acute inflammation in the placenta or amniotic cavity. This study demonstrates that Tc17 cells participate in the pathophysiology of preterm birth, yet further research is required to reveal their specific functions during pregnancy.

Consistent with the human findings, the depletion of Tregs during the third week of pregnancy induced preterm birth that was restored upon the adoptive transfer of such cells. The rates of preterm birth resulting from the depletion of Tregs were modest compared to animal models of systemic and local acute inflammation-induced preterm birth (St Louis et al., 2016; Gomez-Lopez et al., 2016a, 2016b, 2018, 2019; Garcia-Flores et al., 2018). However, this is consistent with the current belief that different subsets of preterm labor and birth are mediated through different mechanisms (Romero et al., 2014a). Thus, in line with this concept, the depletion of Tregs should be responsible only for a subset of idiopathic preterm labors and births. The partial and total depletion of Tregs induced similar rates of preterm birth, which suggests that only a fraction of Tregs need to be depleted to cause preterm birth, regardless of parity. This is relevant to the clinical scenario, in which both nulliparous and multiparous women can present with PTL associated with a reduction of Tregs.

Importantly, the depletion of Tregs induces a fraction of preterm births in the absence of severe systemic acute inflammation, alterations in obstetrical parameters, and intra-amniotic inflammation. These features resemble the clinical scenario of idiopathic PTL (Barros et al., 2015), which is not observed in other established animal models of preterm birth, such as systemic inflammation-induced (Arenas-Hernandez et al., 2019), acute intra-amniotic inflammation-induced (Garcia-Flores et al., 2018; Gomez-Lopez et al., 2018), and progesterone antagonist-induced (Arenas-Hernandez et al., 2019) preterm birth, as well as in another acute inflammatory model (St Louis et al., 2016). Therefore, we surmise that the loss of Tregs is directly implicated in the pathophysiology of this subset of preterm labor/birth. However, the underlying etiologies leading to reduced Tregs, such as dysregulation of the vaginal microbiome (Elovitz et al., 2019; Fettweis et al., 2019) or intestinal microbiome (Shiozaki et al., 2014), require further investigation.

In searching for the mechanisms implicated in this model of idiopathic preterm labor/birth, we found that the depletion of Tregs induced elevated concentrations of CCL7, IL-22, and IFNγ in the maternal circulation. However, only systemic administration of CCL7 and IL-22 at pathological concentrations shortened the length of gestation, inducing early-term delivery. Previous clinical reports have shown that CCL7 (Laudanski et al., 2014) and IL-22 (Bersani et al., 2015) are slightly increased in women with preterm labor and preeclampsia, respectively. Furthermore, the administration of IL-22 reduces Tregs and increases alloreactive Teffs (Zhao et al., 2014). Hence, we propose that the depletion of Tregs shortens the length of gestation by increasing these inflammatory cytokines in the maternal circulation, even though neither the individual nor the combined systemic effects of these cytokines can entirely explain the pathophysiology of preterm birth resulting from the loss of Tregs.

Further investigation revealed that the depletion of Tregs altered specific cellular responses in the maternal circulation, at the maternal-fetal interface, and in the placenta. Overall, Treg depletion increased the abundance of pro-inflammatory immune cells such as B cells (Menard et al., 2007) and neutrophils (Bazzoni et al., 1991) expressing TNF-α and reduced homeostatic immune cells such as arginase 1-expressing neutrophils

(I) Gestational length of cytokine-injected dams. Data are shown as means with standard deviations (n = 3–6 per group).
(J) Rate of early-term or full-term delivery of cytokine-injected dams (n = 3–6 per group).
(K) Percentage of survival from birth until 3 weeks postpartum for neonates born to cytokine-injected dams (n = 3–6 litters per group).
(L–S) Concentrations of (L) IL-6, (M) CXCL10, (N) CCL2, (O) IL-1β, (P) TNF-α, (Q) IFNγ, (R) IL-10, and (S) IL-4 in the amniotic fluid (n = 5–7 per group). Data are shown as medians with interquartile ranges and minimum/maximum ranges.
Statistical analysis was performed using the Mantel-Cox test for survival curves, and Kruskal-Wallis or ANOVA tests with correction for multiple comparisons. See also Figure S5.

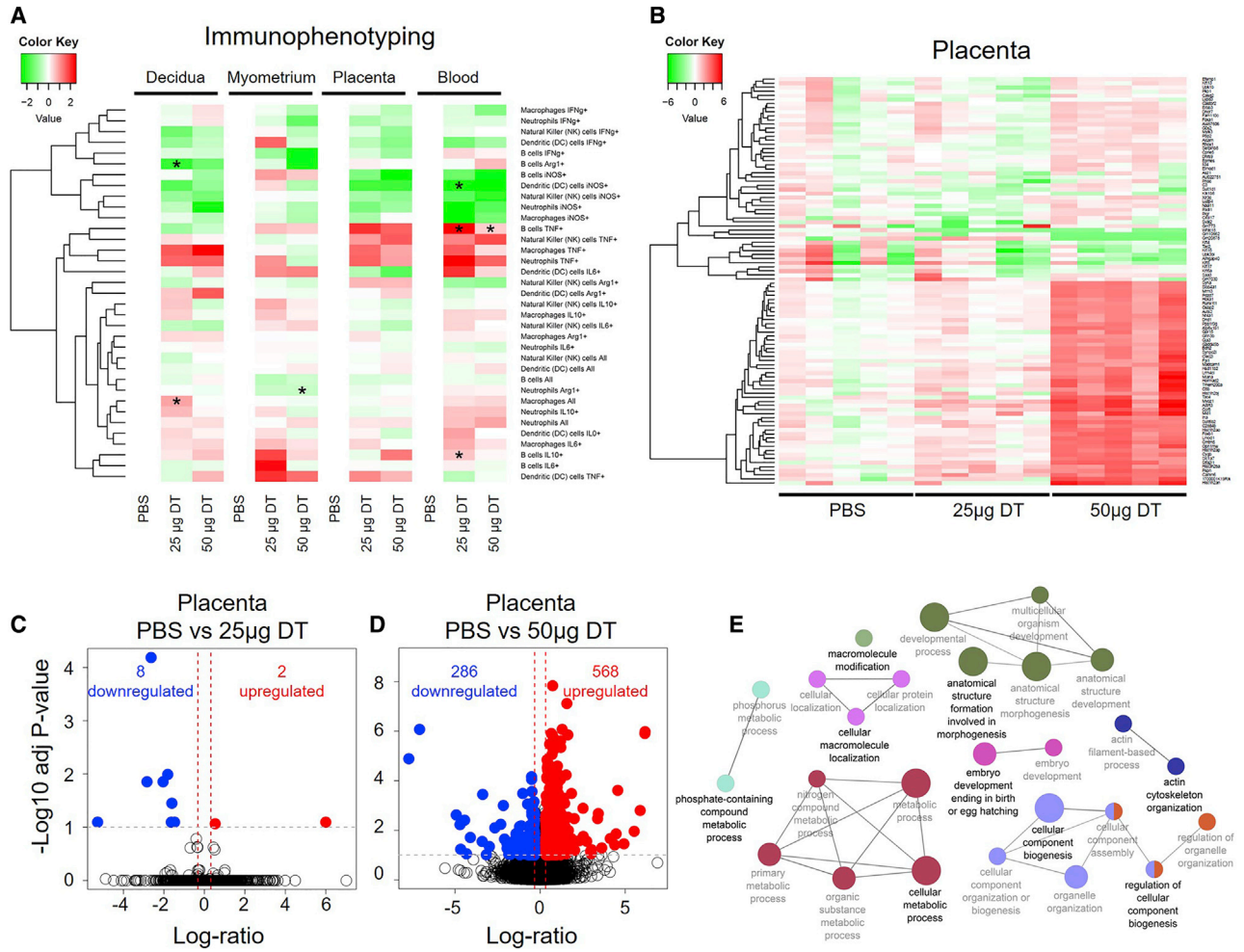

Figure 7. Depletion of Tregs Is Associated with Altered Systemic and Local Cellular Immune Responses and Dysregulation of Developmental and Cellular Processes in the Placenta

Foxp3^{DTR} dams underwent partial or total Treg depletion. Controls were injected with sterile 1× PBS. Mice were euthanized approximately 4 h after the second injection and the decidua, myometrium, placenta, and peripheral blood were collected for flow cytometry (all tissues, n = 5–7 per group) or for RNA-seq analysis (placenta only, n = 5 per group).

(A) Heatmap visualization of changes in the log2-transformed frequencies of immune cell subsets in the decidua, myometrium, placenta, and peripheral blood of partially and totally Treg-depleted *Foxp3*^{DTR} dams relative to controls. Red and green indicate increased and reduced abundance, respectively, relative to PBS controls.

(B) Heatmap visualization of changes in gene expression in the placentas of partially and totally Treg-depleted *Foxp3*^{DTR} dams and controls. Red indicates gene upregulation and green indicates gene downregulation relative to the average value in the PBS group.

(C) Volcano plot showing genes differentially expressed between placentas from partially Treg-depleted *Foxp3*^{DTR} dams and those from control dams.

(D) Volcano plot showing genes differentially expressed between placental tissues from totally Treg-depleted *Foxp3*^{DTR} dams and those from control dams.

(E) Network of biological processes dysregulated in the placentas of totally Treg-depleted *Foxp3*^{DTR} dams.

Statistical analysis was performed using t-tests with false discovery rate adjustment. Asterisks indicate significant differences compared to controls after adjustment. See also Figure S6 and Tables S3, S4, S5, S6, S7, and S8.

(Munder et al., 2006). As expected, IL-10- and TGF-β-expressing CD4+ T cells (i.e., Tregs) were also reduced. Therefore, it is tempting to suggest that Tregs play a central role during late pregnancy in modulating systemic and local cellular responses and that their absence can cause a pro-inflammatory environment, leading to preterm birth.

Importantly, fetuses of Treg-depleted dams exhibited signs of fetal growth restriction, which allowed us to hypothesize that the loss of maternal Tregs causes alterations in placental development. In line with this hypothesis, we found that several key biological processes primarily related to embryo development and cellular metabolic processes were dysregulated in the placental tissues upon Treg depletion. These findings are consistent with previous reports showing that Tregs participate in the development and function of the placenta (Kahn and Baltimore, 2010; Samstein et al., 2012; Loewendorf et al., 2015; Nguyen et al., 2017, 2018; Care et al., 2018). Recently, it was shown that the adoptive transfer of uterine-like NK cells can serve as a treatment

for growth-restricted fetuses (Fu et al., 2017), suggesting that Tregs and NK cells may contribute to the development of offspring.

We also showed that the deleterious effects of Treg depletion on the placenta were carried over to neonatal life, given that a subset of neonates born to Treg-depleted dams died before weaning age. This finding is consistent with clinical studies showing that newborns with growth restriction have fewer cord blood Tregs (Steinborn et al., 2010; Mukhopadhyay et al., 2014). Herein, we also found that adverse neonatal outcomes were more prevalent when Tregs were depleted in repeat pregnancies, supporting the concept that pregnancy imprints protective regulatory memory (Rowe et al., 2012) and that the resulting enhanced Treg expansion in a second pregnancy is involved not only in maternal-fetal tolerance but also in neonatal well-being. Lastly, we provided a causal link between neonatal mortality and Treg depletion since the adoptive transfer of these cells mitigated adverse perinatal outcomes.

In summary, we have shown that a subset of women with idiopathic PTL and birth, formerly considered to have an unknown cause, is associated with a reduction of functional Tregs at the maternal-fetal interface. This finding is in tandem with clinical reports showing that women who underwent preterm labor and birth have reduced numbers and function of Tregs in the maternal circulation (Xiong et al., 2010; Schober et al., 2012). Consistently, the systemic deficiency of Tregs results in a fraction of preterm births in first and repeat pregnancies and, more importantly, induces adverse outcomes in offspring. The mechanisms whereby the loss of Tregs induces adverse perinatal outcomes involve alterations in cellular and soluble immune responses in the mother and at the maternal-fetal interface, as well as dysregulation of developmental and cellular processes in the placenta. This study provides insight into the mechanisms of disease for idiopathic PTL and birth, the leading cause of neonatal morbidity and mortality worldwide.

STAR★METHODS

Detailed methods are provided in the online version of this paper and include the following:

- KEY RESOURCES TABLE
- RESOURCE AVAILABILITY
  - Lead Contact
  - Materials Availability
  - Data and Code Availability
- EXPERIMENTAL MODEL AND SUBJECT DETAILS
  - Human subjects, clinical specimens, and definitions
  - Placental histopathological examination
  - Mice
- METHOD DETAILS
  - Decidual leukocyte isolation from human samples
  - Immunophenotyping of human decidual leukocytes
  - Human Treg suppression assays
  - Treg suppression assays in the second and third week of murine pregnancy
  - Depletion of Tregs in non-pregnant mice and leukocyte isolation from lymphatic tissues
  - Depletion of Tregs in pregnant mice
  - Leukocyte isolation from murine decidua, myometrium, placenta, lymphatic tissues, and peripheral blood to verify Treg depletion
  - Animal models of Treg depletion and preterm birth in the first and second pregnancy
  - Fetal and placental weights from Treg-depleted dams
  - Cell sorting and adoptive transfer of Tregs
  - Measurement of maternal-fetal obstetrical parameters
  - Model of susceptibility to endotoxin-induced preterm birth after Treg depletion
  - Determination of cytokine concentrations in the maternal circulation and amniotic fluid
  - Systemic injection of cytokines/chemokines in pregnant mice
  - Immunophenotyping of leukocytes from the decidual, myometrial, and placental tissues and peripheral blood
  - RNA-seq analysis of placental tissues
- QUANTIFICATION AND STATISTICAL ANALYSIS
  - Statistical Analysis

SUPPLEMENTAL INFORMATION

Supplemental Information can be found online at https://doi.org/10.1016/j.celrep.2020.107874.

ACKNOWLEDGMENTS

We thank the physicians, nurses, and research assistants from the Center for Advanced Obstetrical Care and Research, Intrapartum Unit, Perinatology Research Branch Clinical Laboratory, and Perinatology Research Branch Perinatal Translational Science Laboratory for help with collecting and processing samples. We also thank Tatjana Milovic, Amapola Balancio, Hong Meng, Gaurav Bhatti, and Rebecca Slutsky for help with carrying out some experiments in mice, data analysis, and/or helpful discussion of the findings. This research was supported in part by the Perinatology Research Branch, Division of Obstetrics and Maternal-Fetal Medicine, Division of Intramural Research, *Eunice Kennedy Shriver* National Institute of Child Health and Human Development, National Institutes of Health, U.S. Department of Health and Human Services (NICHD/NIH/DHHS), and in part with federal funds from NICHD/NIH/DHHS under contract HHSN275201300006C. This research was also supported by the Wayne State University Perinatal Initiative in Maternal, Perinatal and Child Health. R.R. contributed to this work as part of his official duties as an employee of the U.S. federal government.

AUTHOR CONTRIBUTIONS

N.G.-L. conceived, designed, and supervised the study. M.A.-H., D.M., Y.L., V.G.-F., Y.X., and J.G. performed the experiments. N.G.-L., M.A.-H., R.R., B.D., A.L.T., D.M., V.G.-F., Y.L., and Y.X. analyzed the data. R.R., S.S.H., and C.-D.H. provided human samples used in the study and intellectual input. H.T. and C.S.-T. provided intellectual input and helpful discussion of the findings. N.G.-L., M.A.-H., D.M., and R.R. wrote the manuscript. All authors revised and provided feedback for the final version of the manuscript.

DECLARATION OF INTERESTS

The authors declare no competing interests.

Received: July 17, 2019
Revised: February 13, 2020
Accepted: June 15, 2020
Published: July 7, 2020

REFERENCES

Aluvihare, V.R., Kallikourdis, M., and Betz, A.G. (2004). Regulatory T cells mediate maternal tolerance to the fetus. Nat. Immunol. *5*, 266–271.

Anders, S., McCarthy, D.J., Chen, Y., Okoniewski, M., Smyth, G.K., Huber, W., and Robinson, M.D. (2013). Count-based differential expression analysis of RNA sequencing data using R and Bioconductor. Nat. Protoc. *8*, 1765–1786.

Arck, P.C., and Hecher, K. (2013). Fetomaternal immune cross-talk and its consequences for maternal and offspring's health. Nat. Med. *19*, 548–556.

Arenas-Hernandez, M., Sanchez-Rodriguez, E.N., Mial, T.N., Robertson, S.A., and Gomez-Lopez, N. (2015). Isolation of Leukocytes from the Murine Tissues at the Maternal-Fetal Interface. J. Vis. Exp. *99*, e52866.

Arenas-Hernandez, M., Romero, R., St Louis, D., Hassan, S.S., Kaye, E.B., and Gomez-Lopez, N. (2016). An imbalance between innate and adaptive immune cells at the maternal-fetal interface occurs prior to endotoxin-induced preterm birth. Cell. Mol. Immunol. *13*, 462–473.

Arenas-Hernandez, M., Romero, R., Xu, Y., Panaitescu, B., Garcia-Flores, V., Miller, D., Ahn, H., Done, B., Hassan, S.S., Hsu, C.D., et al. (2019). Effector and Activated T Cells Induce Preterm Labor and Birth That Is Prevented by Treatment with Progesterone. J. Immunol. *202*, 2585–2608.

Barros, F.C., Papageorghiou, A.T., Victora, C.G., Noble, J.A., Pang, R., Iams, J., Cheikh Ismail, L., Goldenberg, R.L., Lambert, A., Kramer, M.S., et al.; International Fetal and Newborn Growth Consortium for the 21st Century (2015). The distribution of clinical phenotypes of preterm birth syndrome: implications for prevention. JAMA Pediatr. *169*, 220–229.

Bazzoni, F., Cassatella, M.A., Laudanna, C., and Rossi, F. (1991). Phagocytosis of opsonized yeast induces tumor necrosis factor-alpha mRNA accumulation and protein release by human polymorphonuclear leukocytes. J. Leukoc. Biol. *50*, 223–228.

Benjamini, Y., and Hochberg, Y. (1995). Controlling the false discovery rate: a practical and powerful approach to multiple testing. J. R. Stat. Soc. B *57*, 289–300.

Bersani, I., De Carolis, M.P., Foell, D., Weinhage, T., Rossi, E.D., De Carolis, S., Rubortone, S.A., Romagnoli, C., and Speer, C.P. (2015). Interleukin-22: biomarker of maternal and fetal inflammation? Immunol. Res. *61*, 4–10.

Blencowe, H., Cousens, S., Oestergaard, M.Z., Chou, D., Moller, A.B., Narwal, R., Adler, A., Vera Garcia, C., Rohde, S., Say, L., and Lawn, J.E. (2012). National, regional, and worldwide estimates of preterm birth rates in the year 2010 with time trends since 1990 for selected countries: a systematic analysis and implications. Lancet *379*, 2162–2172.

Bonney, E.A. (2016). Immune Regulation in Pregnancy: A Matter of Perspective? Obstet. Gynecol. Clin. North Am. *43*, 679–698.

Bonney, E.A., and Onyekwuluje, J. (2003). The H-Y response in mid-gestation and long after delivery in mice primed before pregnancy. Immunol. Invest. *32*, 71–81.

Burton, G.J., and Jauniaux, E. (2018). Pathophysiology of placental-derived fetal growth restriction. Am. J. Obstet. Gynecol. *218* (*2S*), S745–S761.

Care, A.S., Bourque, S.L., Morton, J.S., Hjartarson, E.P., Robertson, S.A., and Davidge, S.T. (2018). Reduction in Regulatory T Cells in Early Pregnancy Causes Uterine Artery Dysfunction in Mice. Hypertension *72*, 177–187.

Chaouat, G., Voisin, G.A., Escalier, D., and Robert, P. (1979). Facilitation reaction (enhancing antibodies and suppressor cells) and rejection reaction (sensitized cells) from the mother to the paternal antigens of the conceptus. Clin. Exp. Immunol. *35*, 13–24.

Chaouat, G., Kolb, J.P., and Wegmann, T.G. (1983). The murine placenta as an immunological barrier between the mother and the fetus. Immunol. Rev. *75*, 31–60.

Chen, T., Darrasse-Jèze, G., Bergot, A.S., Courau, T., Churlaud, G., Valdivia, K., Strominger, J.L., Ruocco, M.G., Chaouat, G., and Klatzmann, D. (2013). Self-specific memory regulatory T cells protect embryos at implantation in mice. J. Immunol. *191*, 2273–2281.

Cobo, T., Tsiartas, P., Kacerovsky, M., Holst, R.M., Hougaard, D.M., Skogstrand, K., Wennerholm, U.B., Hagberg, H., and Jacobsson, B. (2013). Maternal inflammatory response to microbial invasion of the amniotic cavity: analyses of multiple proteins in the maternal serum. Acta Obstet. Gynecol. Scand. *92*, 61–68.

Combs, C.A., Gravett, M., Garite, T.J., Hickok, D.E., Lapidus, J., Porreco, R., Rael, J., Grove, T., Morgan, T.K., Clewell, W., et al.; ProteoGenix/Obstetrix Collaborative Research Network (2014). Amniotic fluid infection, inflammation, and colonization in preterm labor with intact membranes. Am. J. Obstet. Gynecol. *210*, 125.e1–125.e15.

Couper, K.N., Blount, D.G., de Souza, J.B., Suffia, I., Belkaid, Y., and Riley, E.M. (2007). Incomplete depletion and rapid regeneration of Foxp3+ regulatory T cells following anti-CD25 treatment in malaria-infected mice. J. Immunol. *178*, 4136–4146.

Cox, S.M., Casey, M.L., and MacDonald, P.C. (1997). Accumulation of interleukin-1beta and interleukin-6 in amniotic fluid: a sequela of labour at term and preterm. Hum. Reprod. Update *3*, 517–527.

Cruciani, L., Romero, R., Vaisbuch, E., Kusanovic, J.P., Chaiworapongsa, T., Mazaki-Tovi, S., Dong, Z., Kim, S.K., Ogge, G., Yeo, L., et al. (2010). Pentraxin 3 in maternal circulation: an association with preterm labor and preterm PROM, but not with intra-amniotic infection/inflammation. J. Matern. Fetal Neonatal Med. *23*, 1097–1105.

D'Andrea, A., Aste-Amezaga, M., Valiante, N.M., Ma, X., Kubin, M., and Trinchieri, G. (1993). Interleukin 10 (IL-10) inhibits human lymphocyte interferon gamma-production by suppressing natural killer cell stimulatory factor/IL-12 synthesis in accessory cells. J. Exp. Med. *178*, 1041–1048.

Darrasse-Jèze, G., Klatzmann, D., Charlotte, F., Salomon, B.L., and Cohen, J.L. (2006). CD4+CD25+ regulatory/suppressor T cells prevent allogeneic fetus rejection in mice. Immunol. Lett. *102*, 106–109.

de Waal Malefyt, R., Yssel, H., and de Vries, J.E. (1993). Direct effects of IL-10 on subsets of human CD4+ T cell clones and resting T cells. Specific inhibition of IL-2 production and proliferation. J. Immunol. *150*, 4754–4765.

Deng, W., Yuan, J., Cha, J., Sun, X., Bartos, A., Yagita, H., Hirota, Y., and Dey, S.K. (2019). Endothelial Cells in the Decidual Bed Are Potential Therapeutic Targets for Preterm Birth Prevention. Cell Rep. *27*, 1755–1768.

Doisne, J.M., Balmas, E., Boulenouar, S., Gaynor, L.M., Kieckbusch, J., Gardner, L., Hawkes, D.A., Barbara, C.F., Sharkey, A.M., Brady, H.J., et al. (2015). Composition, Development, and Function of Uterine Innate Lymphoid Cells. J. Immunol. *195*, 3937–3945.

Doncheva, N.T., Morris, J.H., Gorodkin, J., and Jensen, L.J. (2019). Cytoscape StringApp: Network Analysis and Visualization of Proteomics Data. J. Proteome Res. *18*, 623–632.

Dudley, D.J., Hunter, C., Mitchell, M.D., and Varner, M.W. (1997). Amniotic fluid interleukin-10 (IL-10) concentrations during pregnancy and with labor. J. Reprod. Immunol. *33*, 147–156.

Elovitz, M.A., Gajer, P., Riis, V., Brown, A.G., Humphrys, M.S., Holm, J.B., and Ravel, J. (2019). Cervicovaginal microbiota and local immune response modulate the risk of spontaneous preterm delivery. Nat. Commun. *10*, 1305.

Erlebacher, A. (2013). Immunology of the maternal-fetal interface. Annu. Rev. Immunol. *31*, 387–411.

Esplin, M.S., Romero, R., Chaiworapongsa, T., Kim, Y.M., Edwin, S., Gomez, R., Mazor, M., and Adashi, E.Y. (2005). Monocyte chemotactic protein-1 is increased in the amniotic fluid of women who deliver preterm in the presence or absence of intra-amniotic infection. J. Matern. Fetal Neonatal Med. *17*, 365–373.

Fan, M.Y., Low, J.S., Tanimine, N., Finn, K.K., Priyadharshini, B., Germana, S.K., Kaech, S.M., and Turka, L.A. (2018). Differential Roles of IL-2 Signaling in Developing versus Mature Tregs. Cell Rep. *25*, 1204–1213.

Fenton, M.J., Buras, J.A., and Donnelly, R.P. (1992). IL-4 reciprocally regulates IL-1 and IL-1 receptor antagonist expression in human monocytes. J. Immunol. *149*, 1283–1288.

Fettweis, J.M., Serrano, M.G., Brooks, J.P., Edwards, D.J., Girerd, P.H., Parikh, H.I., Huang, B., Arodz, T.J., Edupuganti, L., Glascock, A.L., et al. (2019). The vaginal microbiome and preterm birth. Nat. Med. *25*, 1012–1021.

Figueiredo, A.S., and Schumacher, A. (2016). The T helper type 17/regulatory T cell paradigm in pregnancy. Immunology *148*, 13–21.

Fossiez, F., Djossou, O., Chomarat, P., Flores-Romo, L., Ait-Yahia, S., Maat, C., Pin, J.J., Garrone, P., Garcia, E., Saeland, S., et al. (1996). T cell interleukin-17 induces stromal cells to produce proinflammatory and hematopoietic cytokines. J. Exp. Med. *183*, 2593–2603.

Fu, B., Zhou, Y., Ni, X., Tong, X., Xu, X., Dong, Z., Sun, R., Tian, Z., and Wei, H. (2017). Natural Killer Cells Promote Fetal Development through the Secretion of Growth-Promoting Factors. Immunity *47*, 1100–1113.

Garcia-Flores, V., Romero, R., Miller, D., Xu, Y., Done, B., Veerapaneni, C., Leng, Y., Arenas-Hernandez, M., Khan, N., Panaitescu, B., et al. (2018). Inflammation-Induced Adverse Pregnancy and Neonatal Outcomes Can Be Improved by the Immunomodulatory Peptide Exendin-4. Front. Immunol. *9*, 1291.

Gentleman, R.C., Carey, V.J., Bates, D.M., Bolstad, B., Dettling, M., Dudoit, S., Ellis, B., Gautier, L., Ge, Y., Gentry, J., et al. (2004). Bioconductor: open software development for computational biology and bioinformatics. Genome Biol. *5*, R80.

Gervasi, M.T., Chaiworapongsa, T., Naccasha, N., Blackwell, S., Yoon, B.H., Maymon, E., and Romero, R. (2001). Phenotypic and metabolic characteristics of maternal monocytes and granulocytes in preterm labor with intact membranes. Am. J. Obstet. Gynecol. *185*, 1124–1129.

Gervasi, M.T., Romero, R., Bracalente, G., Erez, O., Dong, Z., Hassan, S.S., Yeo, L., Yoon, B.H., and Chaiworapongsa, T. (2012). Midtrimester amniotic fluid concentrations of interleukin-6 and interferon-gamma-inducible protein-10: evidence for heterogeneity of intra-amniotic inflammation and associations with spontaneous early (<32 weeks) and late (>32 weeks) preterm delivery. J. Perinat. Med. *40*, 329–343.

Gill, N., Leng, Y., Romero, R., Xu, Y., Panaitescu, B., Miller, D., Arif, A., Mumuni, S., Qureshi, F., Hsu, C.D., et al. (2019). The immunophenotype of decidual macrophages in acute atherosis. Am. J. Reprod. Immunol. *81*, e13098.

Goldenberg, R.L., Culhane, J.F., Iams, J.D., and Romero, R. (2008). Epidemiology and causes of preterm birth. Lancet *371*, 75–84.

Gomez-Lopez, N., and Laresgoiti-Servitje, E. (2012). T regulatory cells: regulating both term and preterm labor? Immunol. Cell Biol. *90*, 919–920.

Gomez-Lopez, N., Vega-Sanchez, R., Castillo-Castrejon, M., Romero, R., Cubeiro-Arreola, K., and Vadillo-Ortega, F. (2013). Evidence for a role for the adaptive immune response in human term parturition. Am. J. Reprod. Immunol. *69*, 212–230.

Gomez-Lopez, N., StLouis, D., Lehr, M.A., Sanchez-Rodriguez, E.N., and Arenas-Hernandez, M. (2014). Immune cells in term and preterm labor. Cell. Mol. Immunol. *11*, 571–581.

Gomez-Lopez, N., Romero, R., Arenas-Hernandez, M., Ahn, H., Panaitescu, B., Vadillo-Ortega, F., Sanchez-Torres, C., Salisbury, K.S., and Hassan, S.S. (2016a). *In vivo* T-cell activation by a monoclonal αCD3ε antibody induces preterm labor and birth. Am. J. Reprod. Immunol. *76*, 386–390.

Gomez-Lopez, N., Romero, R., Plazyo, O., Panaitescu, B., Furcron, A.E., Miller, D., Roumayah, T., Flom, E., and Hassan, S.S. (2016b). Intra-Amniotic Administration of HMGB1 Induces Spontaneous Preterm Labor and Birth. Am. J. Reprod. Immunol. *75*, 3–7.

Gomez-Lopez, N., Romero, R., Arenas-Hernandez, M., Schwenkel, G., St Louis, D., Hassan, S.S., and Mial, T.N. (2017a). *In vivo* activation of invariant natural killer T cells induces systemic and local alterations in T-cell subsets prior to preterm birth. Clin. Exp. Immunol. *189*, 211–225.

Gomez-Lopez, N., Romero, R., Plazyo, O., Schwenkel, G., Garcia-Flores, V., Unkel, R., Xu, Y., Leng, Y., Hassan, S.S., Panaitescu, B., et al. (2017b). Preterm labor in the absence of acute histologic chorioamnionitis is characterized by cellular senescence of the chorioamniotic membranes. Am. J. Obstet. Gynecol. *217*, 592.e1–592.e17.

Gomez-Lopez, N., Romero, R., Arenas-Hernandez, M., Panaitescu, B., Garcia-Flores, V., Mial, T.N., Sahi, A., and Hassan, S.S. (2018). Intra-amniotic administration of lipopolysaccharide induces spontaneous preterm labor and birth in the absence of a body temperature change. J. Matern. Fetal Neonatal Med. *31*, 439–446.

Gomez-Lopez, N., Romero, R., Garcia-Flores, V., Leng, Y., Miller, D., Hassan, S.S., Hsu, C.D., and Panaitescu, B. (2019). Inhibition of the NLRP3 inflammasome can prevent sterile intra-amniotic inflammation, preterm labor/birth, and adverse neonatal outcomes. Biol. Reprod. *100*, 1306–1318.

Gousopoulos, E., Proulx, S.T., Bachmann, S.B., Scholl, J., Dionyssiou, D., Demiri, E., Halin, C., Dieterich, L.C., and Detmar, M. (2016). Regulatory T cell transfer ameliorates lymphedema and promotes lymphatic vessel function. JCI Insight *1*, e89081.

Gravett, M.G., Witkin, S.S., Haluska, G.J., Edwards, J.L., Cook, M.J., and Novy, M.J. (1994). An experimental model for intraamniotic infection and preterm labor in rhesus monkeys. Am. J. Obstet. Gynecol. *171*, 1660–1667.

Gustafsson, C., Mjösberg, J., Matussek, A., Geffers, R., Matthiesen, L., Berg, G., Sharma, S., Buer, J., and Ernerudh, J. (2008). Gene expression profiling of human decidual macrophages: evidence for immunosuppressive phenotype. PLoS ONE *3*, e2078.

Hamada, H., Garcia-Hernandez, Mde.L., Reome, J.B., Misra, S.K., Strutt, T.M., McKinstry, K.K., Cooper, A.M., Swain, S.L., and Dutton, R.W. (2009). Tc17, a unique subset of CD8 T cells that can protect against lethal influenza challenge. J. Immunol. *182*, 3469–3481.

Hart, P.H., Vitti, G.F., Burgess, D.R., Whitty, G.A., Piccoli, D.S., and Hamilton, J.A. (1989). Potential antiinflammatory effects of interleukin 4: suppression of human monocyte tumor necrosis factor alpha, interleukin 1, and prostaglandin E2. Proc. Natl. Acad. Sci. USA *86*, 3803–3807.

Heikkinen, J., Möttönen, M., Alanen, A., and Lassila, O. (2004). Phenotypic characterization of regulatory T cells in the human decidua. Clin. Exp. Immunol. *136*, 373–378.

Holt, R., Timmons, B.C., Akgul, Y., Akins, M.L., and Mahendroo, M. (2011). The molecular mechanisms of cervical ripening differ between term and preterm birth. Endocrinology *152*, 1036–1046.

Houser, B.L., Tilburgs, T., Hill, J., Nicotra, M.L., and Strominger, J.L. (2011). Two unique human decidual macrophage populations. J. Immunol. *186*, 2633–2642.

Howson, C.P., Kinney, M.V., McDougall, L., and Lawn, J.E.; Born Too Soon Preterm Birth Action Group (2013). Born too soon: preterm birth matters. Reprod. Health *10* (*Suppl 1*), S1.

Huber, M., Heink, S., Grothe, H., Guralnik, A., Reinhard, K., Elflein, K., Hünig, T., Mittrücker, H.W., Brüstle, A., Kamradt, T., and Lohoff, M. (2009). A Th17-like developmental process leads to CD8(+) Tc17 cells with reduced cytotoxic activity. Eur. J. Immunol. *39*, 1716–1725.

Hunt, J.S., Manning, L.S., and Wood, G.W. (1984). Macrophages in murine uterus are immunosuppressive. Cell. Immunol. *85*, 499–510.

Inada, K., Shima, T., Nakashima, A., Aoki, K., Ito, M., and Saito, S. (2013). Characterization of regulatory T cells in decidua of miscarriage cases with abnormal or normal fetal chromosomal content. J. Reprod. Immunol. *97*, 104–111.

Kahn, D.A., and Baltimore, D. (2010). Pregnancy induces a fetal antigen-specific maternal T regulatory cell response that contributes to tolerance. Proc. Natl. Acad. Sci. USA *107*, 9299–9304.

Kemper, C., Chan, A.C., Green, J.M., Brett, K.A., Murphy, K.M., and Atkinson, J.P. (2003). Activation of human CD4+ cells with CD3 and CD46 induces a T-regulatory cell 1 phenotype. Nature *421*, 388–392.

Kieckbusch, J., Balmas, E., Hawkes, D.A., and Colucci, F. (2015). Disrupted PI3K p110δ Signaling Dysregulates Maternal Immune Cells and Increases Fetal Mortality In Mice. Cell Rep. *13*, 2817–2828.

Kim, J.M., Rasmussen, J.P., and Rudensky, A.Y. (2007). Regulatory T cells prevent catastrophic autoimmunity throughout the lifespan of mice. Nat. Immunol. *8*, 191–197.

Kim, M.J., Romero, R., Kim, C.J., Tarca, A.L., Chhauy, S., LaJeunesse, C., Lee, D.C., Draghici, S., Gotsch, F., Kusanovic, J.P., et al. (2009). Villitis of unknown etiology is associated with a distinct pattern of chemokine up-regulation in the feto-maternal and placental compartments: implications for conjoint maternal

allograft rejection and maternal anti-fetal graft-versus-host disease. J. Immunol. *182*, 3919–3927.

Kim, C.J., Romero, R., Kusanovic, J.P., Yoo, W., Dong, Z., Topping, V., Gotsch, F., Yoon, B.H., Chi, J.G., and Kim, J.S. (2010). The frequency, clinical significance, and pathological features of chronic chorioamnionitis: a lesion associated with spontaneous preterm birth. Mod. Pathol. *23*, 1000–1011.

Kim, C.J., Romero, R., Chaemsaithong, P., Chaiyasit, N., Yoon, B.H., and Kim, Y.M. (2015a). Acute chorioamnionitis and funisitis: definition, pathologic features, and clinical significance. Am. J. Obstet. Gynecol. *213* (*Suppl 4*), S29–S52.

Kim, C.J., Romero, R., Chaemsaithong, P., and Kim, J.S. (2015b). Chronic inflammation of the placenta: definition, classification, pathogenesis, and clinical significance. Am. J. Obstet. Gynecol. *213* (*Suppl 4*), S53–S69.

Kohm, A.P., McMahon, J.S., Podojil, J.R., Begolka, W.S., DeGutes, M., Kasprowicz, D.J., Ziegler, S.F., and Miller, S.D. (2006). Cutting Edge: Anti-CD25 monoclonal antibody injection results in the functional inactivation, not depletion, of CD4+CD25+ T regulatory cells. J. Immunol. *176*, 3301–3305.

Laudanski, P., Lemancewicz, A., Kuc, P., Charkiewicz, K., Ramotowska, B., Kretowska, M., Jasinska, E., Raba, G., Karwasik-Kajszczarek, K., Kraczkowski, J., and Laudanski, T. (2014). Chemokines profiling of patients with preterm birth. Mediators Inflamm. *2014*, 185758.

Lee, J., Romero, R., Xu, Y., Kim, J.S., Topping, V., Yoo, W., Kusanovic, J.P., Chaiworapongsa, T., Hassan, S.S., Yoon, B.H., and Kim, C.J. (2011). A signature of maternal anti-fetal rejection in spontaneous preterm birth: chronic chorioamnionitis, anti-human leukocyte antigen antibodies, and C4d. PLoS ONE *6*, e16806.

Leng, Y., Romero, R., Xu, Y., Galaz, J., Slutsky, R., Arenas-Hernandez, M., Garcia-Flores, V., Motomura, K., Hassan, S.S., Reboldi, A., and Gomez-Lopez, N. (2019). Are B cells altered in the decidua of women with preterm or term labor? Am. J. Reprod. Immunol. *81*, e13102.

Li, Y., Zhang, J., Zhang, D., Hong, X., Tao, Y., Wang, S., Xu, Y., Piao, H., Yin, W., Yu, M., et al. (2017). Tim-3 signaling in peripheral NK cells promotes maternal-fetal immune tolerance and alleviates pregnancy loss. Sci. Signal. *10*, eaah4323.

Liu, L., Oza, S., Hogan, D., Perin, J., Rudan, I., Lawn, J.E., Cousens, S., Mathers, C., and Black, R.E. (2015). Global, regional, and national causes of child mortality in 2000–13, with projections to inform post-2015 priorities: an updated systematic analysis. Lancet *385*, 430–440.

Loewendorf, A.I., Nguyen, T.A., Yesayan, M.N., and Kahn, D.A. (2015). Preeclampsia is Characterized by Fetal NK Cell Activation and a Reduction in Regulatory T Cells. Am. J. Reprod. Immunol. *74*, 258–267.

McGeachy, M.J., Cua, D.J., and Gaffen, S.L. (2019). The IL-17 Family of Cytokines in Health and Disease. Immunity *50*, 892–906.

Menard, L.C., Minns, L.A., Darche, S., Mielcarz, D.W., Foureau, D.M., Roos, D., Dzierszinski, F., Kasper, L.H., and Buzoni-Gatel, D. (2007). B cells amplify IFN-gamma production by T cells via a TNF-alpha-mediated mechanism. J. Immunol. *179*, 4857–4866.

Miller, D., Motomura, K., Garcia-Flores, V., Romero, R., and Gomez-Lopez, N. (2018). Innate Lymphoid Cells in the Maternal and Fetal Compartments. Front. Immunol. *9*, 2396.

Mlecnik, B., Galon, J., and Bindea, G. (2019). Automated exploration of gene ontology term and pathway networks with ClueGO-REST. Bioinformatics *35*, 3864–3866.

Mukhopadhyay, D., Weaver, L., Tobin, R., Henderson, S., Beeram, M., Newell-Rogers, M.K., and Perger, L. (2014). Intrauterine growth restriction and prematurity influence regulatory T cell development in newborns. J. Pediatr. Surg. *49*, 727–732.

Munder, M., Schneider, H., Luckner, C., Giese, T., Langhans, C.D., Fuentes, J.M., Kropf, P., Mueller, I., Kolb, A., Modolell, M., and Ho, A.D. (2006). Suppression of T-cell functions by human granulocyte arginase. Blood *108*, 1627–1634.

Nguyen, T.A., Kahn, D.A., and Loewendorf, A.I. (2017). Maternal-Fetal rejection reactions are unconstrained in preeclamptic women. PLoS ONE *12*, e0188250.

Nguyen, T.A., Kahn, D.A., and Loewendorf, A.I. (2018). Placental implantation over prior cesarean scar causes activation of fetal regulatory T cells. Immun. Inflamm. Dis. *6*, 256–263.

Oh, K.J., Kim, S.M., Hong, J.S., Maymon, E., Erez, O., Panaitescu, B., Gomez-Lopez, N., Romero, R., and Yoon, B.H. (2017). Twenty-four percent of patients with clinical chorioamnionitis in preterm gestations have no evidence of either culture-proven intraamniotic infection or intraamniotic inflammation. Am. J. Obstet. Gynecol. *216*, 604.e1–604.e11.

Onishi, R.M., and Gaffen, S.L. (2010). Interleukin-17 and its target genes: mechanisms of interleukin-17 function in disease. Immunology *129*, 311–321.

Otasek, D., Morris, J.H., Bouças, J., Pico, A.R., and Demchak, B. (2019). Cytoscape Automation: empowering workflow-based network analysis. Genome Biol. *20*, 185.

Paquette, A.G., Brockway, H.M., Price, N.D., and Muglia, L.J. (2018). Comparative transcriptomic analysis of human placentae at term and preterm delivery. Biol. Reprod. *98*, 89–101.

Park, H., Park, K.H., Kim, Y.M., Kook, S.Y., Jeon, S.J., and Yoo, H.N. (2018). Plasma inflammatory and immune proteins as predictors of intra-amniotic infection and spontaneous preterm delivery in women with preterm labor: a retrospective study. BMC Pregnancy Childbirth *18*, 146.

Patro, R., Duggal, G., Love, M.I., Irizarry, R.A., and Kingsford, C. (2017). Salmon provides fast and bias-aware quantification of transcript expression. Nat. Methods *14*, 417–419.

Pereyra, S., Sosa, C., Bertoni, B., and Sapiro, R. (2019). Transcriptomic analysis of fetal membranes reveals pathways involved in preterm birth. BMC Med. Genomics *12*, 53.

Petroff, M.G. (2005). Immune interactions at the maternal-fetal interface. J. Reprod. Immunol. *68*, 1–13.

Pique-Regi, R., Romero, R., Tarca, A.L., Sendler, E.D., Xu, Y., Garcia-Flores, V., Leng, Y., Luca, F., Hassan, S.S., and Gomez-Lopez, N. (2019). Single cell transcriptional signatures of the human placenta in term and preterm parturition. eLife *8*, e52004.

Polanczyk, M.J., Hopke, C., Huan, J., Vandenbark, A.A., and Offner, H. (2005). Enhanced FoxP3 expression and Treg cell function in pregnant and estrogen-treated mice. J. Neuroimmunol. *170*, 85–92.

Poon, L.C., Shennan, A., Hyett, J.A., Kapur, A., Hadar, E., Divakar, H., McAuliffe, F., da Silva Costa, F., von Dadelszen, P., McIntyre, H.D., et al. (2019). The International Federation of Gynecology and Obstetrics (FIGO) initiative on pre-eclampsia: A pragmatic guide for first-trimester screening and prevention. Int. J. Gynaecol. Obstet. *145* (*Suppl 1*), 1–33.

PrabhuDas, M., Bonney, E., Caron, K., Dey, S., Erlebacher, A., Fazleabas, A., Fisher, S., Golos, T., Matzuk, M., McCune, J.M., et al. (2015). Immune mechanisms at the maternal-fetal interface: perspectives and challenges. Nat. Immunol. *16*, 328–334.

Redline, R.W. (2006). Inflammatory responses in the placenta and umbilical cord. Semin. Fetal Neonatal Med. *11*, 296–301.

Redline, R.W., and Patterson, P. (1994). Patterns of placental injury. Correlations with gestational age, placental weight, and clinical diagnoses. Arch. Pathol. Lab. Med. *118*, 698–701.

Redline, R.W., Faye-Petersen, O., Heller, D., Qureshi, F., Savell, V., and Vogler, C.; Society for Pediatric Pathology, Perinatal Section, Amniotic Fluid Infection Nosology Committee (2003). Amniotic infection syndrome: nosology and reproducibility of placental reaction patterns. Pediatr. Dev. Pathol. *6*, 435–448.

Rinaldi, S.F., Makieva, S., Saunders, P.T., Rossi, A.G., and Norman, J.E. (2017). Immune cell and transcriptomic analysis of the human decidua in term and preterm parturition. Mol. Hum. Reprod. *23*, 708–724.

Robertson, S.A., Guerin, L.R., Moldenhauer, L.M., and Hayball, J.D. (2009). Activating T regulatory cells for tolerance in early pregnancy—the contribution of seminal fluid. J. Reprod. Immunol. *83*, 109–116.

Robertson, S.A., Care, A.S., and Moldenhauer, L.M. (2018). Regulatory T cells in embryo implantation and the immune response to pregnancy. J. Clin. Invest. *128*, 4224–4235.

Romero, R., Mazor, M., Wu, Y.K., Sirtori, M., Oyarzun, E., Mitchell, M.D., and Hobbins, J.C. (1988). Infection in the pathogenesis of preterm labor. Semin. Perinatol. *12*, 262–279.

Romero, R., Sirtori, M., Oyarzun, E., Avila, C., Mazor, M., Callahan, R., Sabo, V., Athanassiadis, A.P., and Hobbins, J.C. (1989). Infection and labor. V. Prevalence, microbiology, and clinical significance of intraamniotic infection in women with preterm labor and intact membranes. Am. J. Obstet. Gynecol. *161*, 817–824.

Romero, R., Mazor, M., Sepulveda, W., Avila, C., Copeland, D., and Williams, J. (1992). Tumor necrosis factor in preterm and term labor. Am. J. Obstet. Gynecol. *166*, 1576–1587.

Romero, R., Dey, S.K., and Fisher, S.J. (2014a). Preterm labor: one syndrome, many causes. Science *345*, 760–765.

Romero, R., Miranda, J., Chaiworapongsa, T., Chaemsaithong, P., Gotsch, F., Dong, Z., Ahmed, A.I., Yoon, B.H., Hassan, S.S., Kim, C.J., et al. (2014b). A novel molecular microbiologic technique for the rapid diagnosis of microbial invasion of the amniotic cavity and intra-amniotic infection in preterm labor with intact membranes. Am. J. Reprod. Immunol. *71*, 330–358.

Romero, R., Miranda, J., Chaiworapongsa, T., Korzeniewski, S.J., Chaemsaithong, P., Gotsch, F., Dong, Z., Ahmed, A.I., Yoon, B.H., Hassan, S.S., et al. (2014c). Prevalence and clinical significance of sterile intra-amniotic inflammation in patients with preterm labor and intact membranes. Am. J. Reprod. Immunol. *72*, 458–474.

Romero, R., Grivel, J.C., Tarca, A.L., Chaemsaithong, P., Xu, Z., Fitzgerald, W., Hassan, S.S., Chaiworapongsa, T., and Margolis, L. (2015). Evidence of perturbations of the cytokine network in preterm labor. Am. J. Obstet. Gynecol. *213*, 836.e1–836.e18.

Romero, R., Chaemsaithong, P., Chaiyasit, N., Docheva, N., Dong, Z., Kim, C.J., Kim, Y.M., Kim, J.S., Qureshi, F., Jacques, S.M., et al. (2017). CXCL10 and IL-6: Markers of two different forms of intra-amniotic inflammation in preterm labor. Am. J. Reprod. Immunol. *78*, e12685.

Rowe, J.H., Ertelt, J.M., Aguilera, M.N., Farrar, M.A., and Way, S.S. (2011). Foxp3(+) regulatory T cell expansion required for sustaining pregnancy compromises host defense against prenatal bacterial pathogens. Cell Host Microbe *10*, 54–64.

Rowe, J.H., Ertelt, J.M., Xin, L., and Way, S.S. (2012). Pregnancy imprints regulatory memory that sustains anergy to fetal antigen. Nature *490*, 102–106.

Saito, S., Nakashima, A., Shima, T., and Ito, M. (2010). Th1/Th2/Th17 and regulatory T-cell paradigm in pregnancy. Am. J. Reprod. Immunol. *63*, 601–610.

Salafia, C.M., Vogel, C.A., Vintzileos, A.M., Bantham, K.F., Pezzullo, J., and Silberman, L. (1991). Placental pathologic findings in preterm birth. Am. J. Obstet. Gynecol. *165*, 934–938.

Salvany-Celades, M., van der Zwan, A., Benner, M., Setrajcic-Dragos, V., Bougleux Gomes, H.A., Iyer, V., Norwitz, E.R., Strominger, J.L., and Tilburgs, T. (2019). Three Types of Functional Regulatory T Cells Control T Cell Responses at the Human Maternal-Fetal Interface. Cell Rep. *27*, 2537–2547.

Samstein, R.M., Josefowicz, S.Z., Arvey, A., Treuting, P.M., and Rudensky, A.Y. (2012). Extrathymic generation of regulatory T cells in placental mammals mitigates maternal-fetal conflict. Cell *150*, 29–38.

Sasaki, Y., Sakai, M., Miyazaki, S., Higuma, S., Shiozaki, A., and Saito, S. (2004). Decidual and peripheral blood CD4+CD25+ regulatory T cells in early pregnancy subjects and spontaneous abortion cases. Mol. Hum. Reprod. *10*, 347–353.

Schober, L., Radnai, D., Schmitt, E., Mahnke, K., Sohn, C., and Steinborn, A. (2012). Term and preterm labor: decreased suppressive activity and changes in composition of the regulatory T-cell pool. Immunol. Cell Biol. *90*, 935–944.

Shima, T., Sasaki, Y., Itoh, M., Nakashima, A., Ishii, N., Sugamura, K., and Saito, S. (2010). Regulatory T cells are necessary for implantation and maintenance of early pregnancy but not late pregnancy in allogeneic mice. J. Reprod. Immunol. *85*, 121–129.

Shima, T., Inada, K., Nakashima, A., Ushijima, A., Ito, M., Yoshino, O., and Saito, S. (2015). Paternal antigen-specific proliferating regulatory T cells are increased in uterine-draining lymph nodes just before implantation and in pregnant uterus just after implantation by seminal plasma-priming in allogeneic mouse pregnancy. J. Reprod. Immunol. *108*, 72–82.

Shiozaki, A., Yoneda, S., Yoneda, N., Yonezawa, R., Matsubayashi, T., Seo, G., and Saito, S. (2014). Intestinal microbiota is different in women with preterm birth: results from terminal restriction fragment length polymorphism analysis. PLoS ONE *9*, e111374.

Sindram-Trujillo, A., Scherjon, S., Kanhai, H., Roelen, D., and Claas, F. (2003). Increased T-cell activation in decidua parietalis compared to decidua basalis in uncomplicated human term pregnancy. Am. J. Reprod. Immunol. *49*, 261–268.

Sindram-Trujillo, A.P., Scherjon, S.A., van Hulst-van Miert, P.P., Kanhai, H.H., Roelen, D.L., and Claas, F.H. (2004). Comparison of decidual leukocytes following spontaneous vaginal delivery and elective cesarean section in uncomplicated human term pregnancy. J. Reprod. Immunol. *62*, 125–137.

Slutsky, R., Romero, R., Xu, Y., Galaz, J., Miller, D., Done, B., Tarca, A.L., Gregor, S., Hassan, S.S., Leng, Y., and Gomez-Lopez, N. (2019). Exhausted and Senescent T Cells at the Maternal-Fetal Interface in Preterm and Term Labor. J. Immunol. Res. *2019*, 3128010.

Soneson, C., Love, M.I., and Robinson, M.D. (2015). Differential analyses for RNA-seq: transcript-level estimates improve gene-level inferences. F1000Res. *4*, 1521.

Sorokin, Y., Romero, R., Mele, L., Wapner, R.J., Iams, J.D., Dudley, D.J., Spong, C.Y., Peaceman, A.M., Leveno, K.J., Harper, M., et al. (2010). Maternal serum interleukin-6, C-reactive protein, and matrix metalloproteinase-9 concentrations as risk factors for preterm birth <32 weeks and adverse neonatal outcomes. Am. J. Perinatol. *27*, 631–640.

Sotiriadis, A., Hernandez-Andrade, E., da Silva Costa, F., Ghi, T., Glanc, P., Khalil, A., Martins, W.P., Odibo, A.O., Papageorghiou, A.T., Salomon, L.J., and Thilaganathan, B.; ISUOG CSC Pre-eclampsia Task Force (2019). ISUOG Practice Guidelines: role of ultrasound in screening for and follow-up of pre-eclampsia. Ultrasound Obstet. Gynecol. *53*, 7–22.

St Louis, D., Romero, R., Plazyo, O., Arenas-Hernandez, M., Panaitescu, B., Xu, Y., Milovic, T., Xu, Z., Bhatti, G., Mi, Q.S., et al. (2016). Invariant NKT Cell Activation Induces Late Preterm Birth That Is Attenuated by Rosiglitazone. J. Immunol. *196*, 1044–1059.

Steinborn, A., Engst, M., Haensch, G.M., Mahnke, K., Schmitt, E., Meuer, S., and Sohn, C. (2010). Small for gestational age (SGA) neonates show reduced suppressive activity of their regulatory T cells. Clin. Immunol. *134*, 188–197.

Steinborn, A., Schmitt, E., Kisielewicz, A., Rechenberg, S., Seissler, N., Mahnke, K., Schaier, M., Zeier, M., and Sohn, C. (2012). Pregnancy-associated diseases are characterized by the composition of the systemic regulatory T cell (Treg) pool with distinct subsets of Tregs. Clin. Exp. Immunol. *167*, 84–98.

Svensson, J., Jenmalm, M.C., Matussek, A., Geffers, R., Berg, G., and Ernerudh, J. (2011). Macrophages at the fetal-maternal interface express markers of alternative activation and are induced by M-CSF and IL-10. J. Immunol. *187*, 3671–3682.

Svensson-Arvelund, J., Mehta, R.B., Lindau, R., Mirrasekhian, E., Rodriguez-Martinez, H., Berg, G., Lash, G.E., Jenmalm, M.C., and Ernerudh, J. (2015). The human fetal placenta promotes tolerance against the semiallogeneic fetus by inducing regulatory T cells and homeostatic M2 macrophages. J. Immunol. *194*, 1534–1544.

Tilburgs, T., Roelen, D.L., van der Mast, B.J., van Schip, J.J., Kleijburg, C., de Groot-Swings, G.M., Kanhai, H.H.H., Claas, F.H.J., and Scherjon, S.A. (2006). Differential distribution of CD4(+)CD25(bright) and CD8(+)CD28(−) T-cells in decidua and maternal blood during human pregnancy. Placenta *27* (*Suppl A*), S47–S53.

Tilburgs, T., Roelen, D.L., van der Mast, B.J., de Groot-Swings, G.M., Kleijburg, C., Scherjon, S.A., and Claas, F.H. (2008). Evidence for a selective migration of fetus-specific CD4+CD25bright regulatory T cells from the peripheral blood to the decidua in human pregnancy. J. Immunol. *180*, 5737–5745.

Tsuda, S., Zhang, X., Hamana, H., Shima, T., Ushijima, A., Tsuda, K., Muraguchi, A., Kishi, H., and Saito, S. (2018). Clonally Expanded Decidual Effector Regulatory T Cells Increase in Late Gestation of Normal Pregnancy, but Not in Preeclampsia, in Humans. Front. Immunol. *9*, 1934.

Tsuda, S., Nakashima, A., Shima, T., and Saito, S. (2019). New Paradigm in the Role of Regulatory T Cells During Pregnancy. Front. Immunol. *10*, 573.

Vacca, P., Montaldo, E., Croxatto, D., Loiacono, F., Canegallo, F., Venturini, P.L., Moretta, L., and Mingari, M.C. (2015). Identification of diverse innate lymphoid cells in human decidua. Mucosal Immunol. *8*, 254–264.

van der Zwan, A., Bi, K., Norwitz, E.R., Crespo, A.C., Claas, F.H.J., Strominger, J.L., and Tilburgs, T. (2018). Mixed signature of activation and dysfunction allows human decidual $CD8^+$ T cells to provide both tolerance and immunity. Proc. Natl. Acad. Sci. USA *115*, 385–390.

Wei, X., Zhang, J., Gu, Q., Huang, M., Zhang, W., Guo, J., and Zhou, X. (2017). Reciprocal Expression of IL-35 and IL-10 Defines Two Distinct Effector Treg Subsets that Are Required for Maintenance of Immune Tolerance. Cell Rep. *21*, 1853–1869.

Willcockson, A.R., Nandu, T., Liu, C.L., Nallasamy, S., Kraus, W.L., and Mahendroo, M. (2018). Transcriptome signature identifies distinct cervical pathways induced in lipopolysaccharide-mediated preterm birth. Biol. Reprod. *98*, 408–421.

Xiong, H., Zhou, C., and Qi, G. (2010). Proportional changes of CD4+CD25+Foxp3+ regulatory T cells in maternal peripheral blood during pregnancy and labor at term and preterm. Clin. Invest. Med. *33*, E422.

Xu, Y., Plazyo, O., Romero, R., Hassan, S.S., and Gomez-Lopez, N. (2015). Isolation of Leukocytes from the Human Maternal-fetal Interface. J. Vis. Exp. *99*, e52863.

Xu, Y., Romero, R., Miller, D., Kadam, L., Mial, T.N., Plazyo, O., Garcia-Flores, V., Hassan, S.S., Xu, Z., Tarca, A.L., et al. (2016). An M1-like Macrophage Polarization in Decidual Tissue during Spontaneous Preterm Labor That Is Attenuated by Rosiglitazone Treatment. J. Immunol. *196*, 2476–2491.

Xu, Y., Romero, R., Miller, D., Silva, P., Panaitescu, B., Theis, K.R., Arif, A., Hassan, S.S., and Gomez-Lopez, N. (2018). Innate lymphoid cells at the human maternal-fetal interface in spontaneous preterm labor. Am. J. Reprod. Immunol. *79*, e12820.

Yao, Z., Painter, S.L., Fanslow, W.C., Ulrich, D., Macduff, B.M., Spriggs, M.K., and Armitage, R.J. (1995). Human IL-17: a novel cytokine derived from T cells. J. Immunol. *155*, 5483–5486.

Yellon, S.M. (2017). Contributions to the dynamics of cervix remodeling prior to term and preterm birth. Biol. Reprod. *96*, 13–23.

Yoon, B.H., Romero, R., Moon, J.B., Shim, S.S., Kim, M., Kim, G., and Jun, J.K. (2001). Clinical significance of intra-amniotic inflammation in patients with preterm labor and intact membranes. Am. J. Obstet. Gynecol. *185*, 1130–1136.

Zenclussen, A.C., Gerlof, K., Zenclussen, M.L., Sollwedel, A., Bertoja, A.Z., Ritter, T., Kotsch, K., Leber, J., and Volk, H.D. (2005). Abnormal T-cell reactivity against paternal antigens in spontaneous abortion: adoptive transfer of pregnancy-induced CD4+CD25+ T regulatory cells prevents fetal rejection in a murine abortion model. Am. J. Pathol. *166*, 811–822.

Zhao, K., Zhao, D., Huang, D., Yin, L., Chen, C., Pan, B., Wu, Q., Li, Z., Yao, Y., Shen, E., et al. (2014). Interleukin-22 aggravates murine acute graft-versus-host disease by expanding effector T cell and reducing regulatory T cell. J. Interferon Cytokine Res. *34*, 707–715.

STAR★METHODS

KEY RESOURCES TABLE

REAGENT or RESOURCE	SOURCE	IDENTIFIER
Antibodies		
CD45-AlexaFluor700; Clone HI30	BD Biosciences	Cat# 560566; RRID:AB_1645452
CD3-APC-Cy7; Clone SK7	BD Biosciences	Cat# 557832; RRID:AB_396890
CD4-PE-CF594; Clone RPA-T4	BD Biosciences	Cat# 562316; RRID:AB_11154394
CD8-PE; Clone RPA-T8	BD Biosciences	Cat# 561949; RRID:AB_10897146
CD25-PE-Cy7; Clone M-A251	BD Biosciences	Cat# 557741; RRID:AB_396847
FoxP3-V450; Clone 259D/C7	BD Biosciences	Cat# 560459; RRID:AB_1645591
IL-17A-AlexaFluor488; Clone N49-653	BD Biosciences	Cat# 560489; RRID:AB_1645355
IgG1, κ Isotype Control-V450; Clone MOPC-21	BD Biosciences	Cat# 560373; RRID:AB_1645606
IgG2b, κ Isotype Control-AlexaFluor 488; Clone 27-35	BD Biosciences	Cat# 558716; RRID:AB_1645613
CD3-APC-Cy7; Clone 145-2C11	BD Biosciences	Cat# 557596; RRID:AB_396759
CD4-APC; Clone RM4-5	BD Biosciences	Cat# 553051; RRID:AB_398528
CD8-PE-CF594; Clone 53-6.7	BD Biosciences	Cat# 562283; RRID:AB_11152075
CD25-PE; Clone 7D4	Miltenyi Biotec	Cat# 130-118-550; RRID:AB_2784088
Foxp3-V450; Clone MF23	BD Biosciences	Cat# 561293; RRID:AB_10611728
CD45-AF700; Clone 30-F11	BD Biosciences	Cat# 560510; RRID:AB_1645208
CD11b-BV737; Clone M1/70	BD Biosciences	Cat# 564443; RRID:AB_2738811
F4/80-APC-eFluor780; Clone BM8	eBioscience	Cat# 12-4801-82; RRID:AB_465923
Ly6G-BV395; Clone 1A8	BD Biosciences	Cat# 563978; RRID:AB_2716852
CD11c-BV711; Clone HL3	BD Biosciences	Cat# 563048; RRID:AB_2734778
CD49b-PE-CF594; Clone DX5	BD Biosciences	Cat# 562453; RRID:AB_11153857
CD19-BV421; Clone 1D3	BD Biosciences	Cat# 562701; RRID:AB_2737731
CD205-PerCP eFluor710; Clone 205yekta	eBioscience	Cat# 46-2051-82; RRID:AB_1834423
iNOS-PE; Clone CXNFT	eBioscience	Cat # 12-5920-82; RRID:AB_2572642
Arg1-FITC; Polyclonal	R&D Systems	Cat # IC5868F; RRID:AB_10718118
IFNγ-BV786; Clone XMG1.2	BD Biosciences	Cat# 563773; RRID:AB_2738419
IL10-BV605; Clone JES5-16E3	BD Biosciences	Cat# 564082; RRID:AB_2738582
TNFα-PECy7; Clone MP6-XT22	BD Biosciences	Cat# 557644; RRID:AB_396761
IL6-APC; Clone MP5-20F3	BD Biosciences	Cat# 561367; RRID:AB_10679354
CD3-BV650; Clone 145-2C11	BD Biosciences	Cat# 564378; RRID:AB_2738779
CD4-PECy5; Clone RM4-5	BD Biosciences	Cat# 553050; RRID:AB_394586
CD8-APC-Cy7; Clone 53-6.7	BD Biosciences	Cat# 557654; RRID:AB_396769
CD25-BV711; Clone PC61	BD Biosciences	Cat# 740714; RRID:AB_2740396
IL2-AF700; Clone JES6-5H4	BD Biosciences	Cat# 561287; RRID:AB_10679118
IL4-BV421; Clone 11B11	BD Biosciences	Cat# 562915; RRID:AB_2737889
Foxp3-AF488; Clone MF23	BD Biosciences	Cat# 560403; RRID:AB_1645192
IL17A-BV786; Clone TC11-18H10	BD Biosciences	Cat# 564171; RRID:AB_2738642
IgG2a, κ Isotype Control-PE; Clone eBR2a	eBioscience	Cat# 12-4321-80; RRID:AB_1834380
IgG Control-FITC; Polyclonal	R&D Systems	Cat# IC016F; RRID:AB_1267476
IgG1, κ Isotype Control-BV786; Clone R3-34	BD Biosciences	Cat# 563847; RRID:N/A
IgG2b, κ Isotype Control-BV605; Clone R35-38	BD Biosciences	Cat# 563145; RRID:N/A
IgG1, κ Isotype Control-PE-Cy7; Clone R3-34	BD Biosciences	Cat# 557645; RRID:AB_396762
IgG1, κ Isotype Control-APC; Clone R3-34	BD Biosciences	Cat# 554686; RRID:AB_39857
IgG1, κ Isotype Control-BV421; Clone R3-34	BD Biosciences	Cat# 562868; RRID:AB_2734711

(*Continued on next page*)

Continued

REAGENT or RESOURCE	SOURCE	IDENTIFIER
IgG2b, κ Isotype Control AF488; Clone A95-1	BD Biosciences	Cat# 557726; RRID:AB_396834
CD45-APC-Cy7; Clone 2D1	BD Biosciences	Cat# 557833, RRID: AB_396891
CD3-PerCP-Cy5.5; Clone SK7	BD Biosciences	Cat# 340949, RRID: AB_400190
CD4-BUV737; Clone SK3	BD Biosciences	Cat# 564305, RRID: AB_2713927
CD8-BUV395; Clone RPA-T8	BD Biosciences	Cat# 563795, RRID: AB_2722501
CD25-PE-Cy7; Clone M-A251	BD Biosciences	Cat# 557741, RRID: AB_396847
IL-17A-BV650; Clone N49-653	BD Biosciences	Cat# 563746, RRID: AB_2738402
IgG1, κ Isotype Control-BV650; Clone X40	BD Biosciences	Cat# 563231, RRID: N/A
FoxP3-Alexa Fluor 647; Clone 295DD/C7	BD Biosciences	Cat# 560045, RRID: AB_1645411
IgG1, κ Isotype Control-Alexa Fluor 647; Clone MOPC-21	BD Biosciences	Cat# 557714, RRID: AB_396823
FoxP3-Alexa Fluor 488; Clone 295DD/C7	BD Biosciences	Cat# 560047, RRID: AB_1645349
IgG1, κ Isotype Control-Alexa Fluor 488; Clone MOPC-21	BD Biosciences	Cat# 557702, RRID: AB_396811
Biological Samples		
Human placental basal plate (decidua basalis) and chorioamniotic membrane (decidua parietalis) samples	Perinatology Research Branch, an intramural program of the *Eunice Kennedy Shriver* NICHD, NIH, DHHS, Wayne State University (Detroit, MI, USA), and the Detroit Medical Center (Detroit, MI, USA)	N/A
Chemicals, Peptides, and Recombinant Proteins		
Diphtheria toxin (*Corynebacterium diptheriae*)	Sigma-Aldrich	Cat# D0564
Diphtheria toxin (*Corynebacterium diptheriae*)	Calbiochem, EMD Millipore Corp	Cat# 322326-1MG
Diphtheria toxin (*Corynebacterium diptheriae*)	Enzo Life Sciences	Cat# BML-G135
Lipopolysaccharides from *Escherichia coli* O55:B5	Sigma-Aldrich	Cat# L6259-1MG
BD Horizon Fixable Viability Stain 510	BD Biosciences	Cat# 564406
BD Horizon Fixable Viability Stain 575V	BD Biosciences	Cat# 565694
LIVE/DEAD Fixable Green Dead Cell Stain Kit	Invitrogen, Thermo Fisher Scientific	Cat# L23101
CellTrace Violet Cell Proliferation Kit	Molecular Probes, Thermo Fisher Scientific	Cat# C34557
IL2 Recombinant Human Protein	GIBCO, Thermo Fisher Scientific	Cat# PHC0026
2-Mercaptoethanol	GIBCO, Thermo Fisher Scientific	Cat# 21985-023
Mouse IL-2	Miltenyi Biotec	Cat# 130-094-054
Animal Free Recombinant Mouse IFNγ	PeproTech	Cat# AF-315-05
Recombinant Mouse CCL7	R&D Systems	Cat# 456-MC-010/CF
Recombinant Mouse IL-22	Biolegend	Cat# 576202
Deposited Data		
RNA-Seq data of murine placental tissues	This manuscript	GEO: GSE145357
Experimental Models: Organisms/Strains		
B6.129(Cg)-*Foxp3*$^{tm3(DTR/GFP)Ayr}$ (*Foxp3*^{DTR})	The Jackson Laboratory	Stock# 016958
C57BL/6-Tg (CAG-EGFP)131Osb/LeySopJ (*EGFP*)	The Jackson Laboratory	Stock# 006567
C57BL/6	The Jackson Laboratory	Stock# 000664
BALB/cBy	The Jackson Laboratory	Stock# 001026
Other		
Stain buffer	BD Biosciences	Cat# 554656
Foxp3/Transcription Factor Fixation/ Permeabilization solution	eBioscience	Cat# 00-5523-00
CD4+ CD25+ Regulatory T Cell Isolation Kit, mouse	Miltenyi Biotec	Cat# 130-091-041

(*Continued on next page*)

Continued

REAGENT or RESOURCE	SOURCE	IDENTIFIER
Treg Expansion Kit, mouse (CD3/CD28 MACSiBead particles)	Miltenyi Biotec	Cat# 130-095-925
Dynabeads Human T-Activator CD3/CD28 for T Cell Expansion and Activation	GIBCO, Thermo Fisher Scientific	Cat# 11161D
ProcartaPlex Mouse Cytokine & Chemokine Panel 1A 36-plex	ThermoFisher	Cat# EPX360-26092-901

RESOURCE AVAILABILITY

Lead Contact

Further information and requests for resources and reagents should be directed to and will be fulfilled by the lead contact, Nardhy Gomez-Lopez (nardhy.gomez-lopez@wayne.edu).

Materials Availability

This study did not generate new unique reagents.

Data and Code Availability

The accession number for the RNA-seq data reported in this paper is GEO: GSE145357.

EXPERIMENTAL MODEL AND SUBJECT DETAILS

Human subjects, clinical specimens, and definitions

Human placental basal plate (decidua basalis) and chorioamniotic membrane (decidua parietalis) samples were obtained at the Perinatology Research Branch, an intramural program of the *Eunice Kennedy Shriver* National Institute of Child Health and Human Development (NICHD), National Institutes of Health, U.S. Department of Health and Human Services, Wayne State University (Detroit, MI, USA), and the Detroit Medical Center (Detroit, MI, USA). The collection and use of human materials for research purposes were approved by the Institutional Review Boards of NICHD and Wayne State University. All participating women provided written informed consent prior to sample collection. The study groups included women who delivered at term with labor/birth (TIL), at term without labor (TNL), preterm with labor (PTL), or preterm without labor (PTNL). Patients with PTL were further categorized into those who underwent idiopathic preterm labor/birth without inflammation (iPTL), those with idiopathic preterm labor/birth with chronic inflammatory lesions of the placenta (iPTL+CI), and those with preterm labor/birth with acute inflammatory lesions of the placenta (PTL+AI). Patients with TIL were further categorized into those who underwent term labor without inflammation (TIL), those with chronic inflammatory lesions of the placenta (TIL+CI), and those with acute inflammatory lesions of the placenta (TIL+AI). The demographic and clinical characteristics of the study groups are shown in Tables S1 and S2. Labor was defined by the presence of regular uterine contractions at a frequency of at least two contractions every 10 min with cervical changes resulting in delivery. Preterm delivery was defined as delivery < 37 weeks of gestation. Patients with multiple births or neonates that had congenital or chromosomal abnormalities were excluded from this study.

Placental histopathological examination

Placentas were examined histologically by a perinatal pathologist blinded to clinical diagnoses and obstetrical outcomes according to standardized Perinatology Research Branch protocols. Briefly, three to nine sections of the placenta were examined, and at least one full-thickness section was taken from the center of the placenta; others were taken randomly from the placental disc. Chronic and acute inflammatory lesions of the placenta were diagnosed following established Perinatology Research Branch protocols (Redline et al., 2003, Redline, 2006, Kim et al., 2015a, 2015b).

Mice

B6.129(Cg)-Foxp3$^{tm3(DTR/GFP)Ayr}$ (*Foxp3*^{DTR}), BALB/cBy (BALB/c), C57BL/6-Tg (CAG-EGFP)131Osb/LeySopJ (*EGFP*), and C57BL/6 mice were purchased from The Jackson Laboratory (Bar Harbor, ME, USA). Mice were bred in the animal care facility at the C.S. Mott Center for Human Growth and Development (Wayne State University, Detroit, MI, USA) and housed under a circadian cycle (light:-dark = 12:12 h). Eight- to twelve-week-old *Foxp3*^{DTR}, *EGFP*, or C57BL/6 females were mated with BALB/c or C57BL/6 males of proven fertility. Female mice were examined daily between 8:00 and 9:00 a.m. for the presence of a vaginal plug, which indicated 0.5 days *post coitum* (dpc). After observation of vaginal plugs, female mice were removed from the mating cages and housed separately. A weight gain $\geq$ 2 g confirmed pregnancy at 12.5 dpc. All animal experiments were approved by the Institutional Animal Care and Use Committee at Wayne State University (Protocol No: A-09-08-12, A-07-03-15 and 18-03-0584).

METHOD DETAILS

Decidual leukocyte isolation from human samples

Leukocytes were isolated from human decidual tissue (Table S2) as previously described (Xu et al., 2015). Briefly, the decidua basalis was collected from the basal plate of the placenta, and the decidua parietalis was separated from the chorioamniotic membranes. Decidual tissue was homogenized using a gentleMACS Dissociator (Miltenyi Biotec, San Diego, CA, USA) in StemPro Cell Dissociation Reagent (Life Technologies, Grand Island, NY, USA). Homogenized tissues were incubated for 45 min at 37°C with gentle agitation. After incubation, tissues were washed with 1X PBS (Life Technologies) and filtered through a 100 μm cell strainer. Cell suspensions were collected and centrifuged at 300 x g for 10 min at 4°C, and the cell pellet was suspended in stain buffer (BD Biosciences, San Jose, CA, USA). Mononuclear cells were purified using a density gradient (Ficoll-Paque Plus; GE Healthcare Bio-Sciences, Uppsala, Sweden), following the manufacturer's instructions. Then, mononuclear cell suspensions were washed using stain buffer prior to immunophenotyping.

Immunophenotyping of human decidual leukocytes

Mononuclear cell suspensions were washed with stain buffer and centrifuged. Cell pellets were incubated for 10 min at 4°C with 20 μL of human FcR Blocking Reagent (Miltenyi Biotec) in 80 μL of stain buffer. Next, mononuclear cell suspensions were incubated with extracellular fluorochrome-conjugated anti-human mAbs (Key Resources Table) for 30 min at 4°C in the dark. After extracellular staining, the cells were fixed. For intracellular staining, the cells were fixed and permeabilized using the Foxp3/Transcription Factor Fixation/Permeabilization solution (eBioscience) prior to incubation with intracellular anti-human mAbs (Key Resources Table). Finally, mononuclear cell suspensions were washed and resuspended in 0.5 mL of stain buffer and acquired using the BD LSR Fortessa flow cytometer and FACSDiva 6.0 software. Flow cytometry analysis was performed using the FlowJo software v10 (FlowJo, Ashland, OR, USA).

Human Treg suppression assays

Decidual leukocytes were isolated from the decidual basalis from women who delivered preterm or at term (Table S1), as described above. Leukocytes were incubated with BD Horizon Fixable Viability Stain 510 for 30 min at 4°C, then washed with 1X PBS. The cells were resuspended in stain buffer and incubated with fluorochrome conjugated anti-human mAbs (Key Resources Table) for 30 min at 4°C in the dark. The cells were washed with 1X PBS to remove excess antibody, resuspended in 0.5 mL of presort buffer (BD Biosciences), and effector T cells (Teff cells; CD45+CD3+CD4+CD25- cells) and regulatory T cells (Tregs; CD45+CD3+CD4+CD25+CD127low cells) were sorted using the BD FACSMelody cell sorter (BD Biosciences) and BD FACSChorus version 1.3 software (BD Biosciences). The expression of Foxp3 by sorted Tregs was confirmed by flow cytometry using the BD LSR Fortessa flow cytometer and FACSDiva 6.0 software.

Sorted Tregs were resuspended in RPMI media (Thermo Fisher Scientific, Grand Island, NY, USA) supplemented with 10% FBS and 1% penicillin/streptomycin (Thermo Fisher Scientific) at $4x10^4$ cells/mL. Purified CD4+CD25- Teff cells were labeled with the CellTrace Violet Cell Proliferation Kit (Molecular Probes, Eugene, OR, USA), following the manufacturer's instructions. Labeled Teff cells were adjusted to $4x10^4$ cells/mL in supplemented RPMI medium. The Tregs and Teff cells were co-cultured in a round-bottom 96-well plate at a ratio of 1:1, 1:2, 1:4, and 1:8, respectively. Dynabeads Human T-Activator CD3/CD28 were added to the co-culture to obtain a bead:cell ratio of 1:1. The culture plate was then incubated at 37°C with 5% CO_2 for 96 h. Human recombinant IL-2 (30 U/mL; Thermo Fisher Scientific) was used to stimulate T cell expansion, and 2-mercaptoethanol (55 μM; Thermo Fisher Scientific) was added to maintain cell viability. The suppressive capacity of Treg cells was determined using flow cytometry to analyze the proliferation of Teff cells under different co-culture conditions, according to the CellTrace Violet fluorescence intensity of the Teff cells. The percentage of Treg suppression of Teff cell expansion was calculated using the following formula: percentage of suppression = [(Number of proliferated Teff cells cultured alone – Number of proliferated Teff cells co-cultured with Tregs)/Number proliferated Teff cells cultured alone] x 100.

Treg suppression assays in the second and third week of murine pregnancy

C57BL/6 female mice were mated with BALB/c males as described above. Dams were sacrificed either in the 2nd week (10.5-13.5 dpc) or 3rd week (16.5 dpc) of pregnancy and the spleens were harvested. Splenocytes were isolated from the spleen as previously described (Arenas-Hernandez et al., 2016), filtered through a 30 μm cell strainer (Miltenyi Biotec), and washed with sterile 1X PBS. Splenocytes were counted using an automatic cell counter (Cellometer Auto 2000; Nexcelom, Lawrence, MA, USA) to obtain a preliminary cell number for Treg isolation. Approximately $1x10^8$ splenocytes were taken for Treg isolation using the mouse CD4+CD25+ Regulatory T cell Isolation Kit (Miltenyi Biotec), following the manufacturer's instructions. The counts of isolated Tregs (CD3+CD4+CD25+Foxp3+ cells) and Teff (CD3+CD4+CD25- cells) cells were determined by flow cytometry, using CountBright Absolute Counting Beads (Molecular Probes).

Purified Tregs were adjusted to $5x10^5$ cells/mL in supplemented RPMI. Purified Teff cells were labeled with the CellTrace Violet Cell Proliferation Kit, following the manufacturer's instructions. Labeled Teff cells were adjusted to $5x10^5$ cells/mL in supplemented RPMI medium. The Tregs and Teff cells were co-cultured in a round-bottom 96-well plate at a ratio of 1:1, 1:2, 1:4, and 1:8, respectively, and cultured with CD3/CD28-loaded MACSiBeads ($5x10^5$ beads/mL), mouse recombinant IL-2 (200 U/mL; Miltenyi Biotec), and 2-mer-

captoethanol (55μM). The culture plate was then incubated at 37°C with 5% CO_2 for 96 h. The suppressive capacity of Tregs was determined using flow cytometry to analyze the proliferation of Teff cells under different co-culture conditions, according to the CellTrace Violet fluorescence intensity of the Teff cells. Dead cells were excluded using the Live/Dead Fixable Green Dead Cell Stain Kit (Molecular Probes). The percentage of Treg suppression of Teff cell expansion was calculated using the following formula: percentage of suppression = [(Number of proliferated Teff cells cultured alone – Number of proliferated Teff cells co-cultured with Tregs)/ Number proliferated Teff cells cultured alone] x 100.

Depletion of Tregs in non-pregnant mice and leukocyte isolation from lymphatic tissues

Naive non-pregnant *Foxp3*^{DTR} mice were injected intraperitoneally (i.p.) with 25 μg/kg (partial depletion of Tregs) or 50 μg/kg (total depletion of Tregs) of diphtheria toxin from *Corynebacterium diphtheria* (DT; Sigma-Aldrich, St. Louis, MO, USA; Calbiochem, EMD Millipore Corp, Billerica, MA, USA; or Enzo Life Sciences, Inc., Farmingdale, NY, USA) in 200 μL of sterile 1X PBS (Fisher Scientific, Fair Lawn, NY, USA) or with 200 μL sterile 1X PBS using a 26-gauge needle. Twenty-four hours post-injection, mice received a second injection of 25 or 50 μg/kg of DT, respectively, in 200 μL of sterile 1X PBS, or with 200 μL sterile 1X PBS. Four hours later, the uterine-draining lymph nodes (ULN), spleen, and thymus were collected and leukocyte suspensions were prepared as previously reported (Arenas-Hernandez et al., 2016) to determine the proportion of Tregs (CD3+CD4+CD25+Foxp3+ cells) by flow cytometry.

Depletion of Tregs in pregnant mice

Foxp3^{DTR} dams were injected i.p. with 25 μg/kg of DT (Rowe et al., 2011, 2012) (partial depletion of Tregs) or 50 μg/kg of DT (Kim et al., 2007, Samstein et al., 2012) (total depletion of Tregs) dissolved in 200 μL of sterile 1X PBS using a 26-gauge needle on 14.5 dpc. Controls were injected with 200 μL of sterile 1X PBS alone. After 24 h, dams were injected with 5 μg/kg of DT or 50 μg/kg of DT, respectively, in 200 μL of sterile 1X PBS, or with 200 μL of sterile 1X PBS alone. Four hours later, dams were euthanized and the decidual, myometrial, placental, and lymphatic tissues were collected, as well as the peripheral blood, to determine the proportion of Tregs by flow cytometry.

Leukocyte isolation from murine decidua, myometrium, placenta, lymphatic tissues, and peripheral blood to verify Treg depletion

Isolation of leukocytes from decidual, myometrial, and placental tissues was performed as previously described (Arenas-Hernandez et al., 2015). Briefly, tissues were minced into small pieces using fine scissors and enzymatically digested with StemPro Cell Dissociation Reagent for 35 minutes at 37°C. Peripheral blood mononuclear cells (PBMCs) were isolated by density gradient using Ficoll-Paque Plus and washed with 1X PBS. The uterine-draining lymph nodes (ULN), inguinal lymph nodes (ILN), mesenteric lymph nodes (MLN), spleen, and thymus were also collected and leukocyte suspensions were prepared, as previously reported (Arenas-Hernandez et al., 2016). Leukocytes were filtered using a 100 μm cell strainer and washed with FACS buffer [0.1% BSA (Sigma-Aldrich) and 0.05% sodium azide (Fisher Scientific Chemicals) in 1X PBS)] before immunophenotyping.

Leukocyte suspensions prepared from the decidua, myometrium, placenta, lymphatic tissues, and peripheral blood were centrifuged at 1,250 x g for 10 min at 4°C in the dark. Cells were stained with the Live/Dead Fixable Green Dead Cell Stain Kit for 10 min at 4°C in the dark, followed by washing with 1X PBS. Cell pellets were then incubated with the CD16/CD32 mAb (FcγIII/II receptor; BD Biosciences) for 10 min and subsequently incubated with specific fluorochrome-conjugated anti-mouse mAbs (Key Resources Table) for 30 min at 4°C in the dark. Leukocyte suspensions were fixed/permeabilized with the Foxp3/Transcription Factor Staining Buffer Set (eBioscience) prior to staining with intranuclear anti-mouse mAbs. Cells were acquired for determination of Tregs (CD3+CD4+CD25+Foxp3+ cells) using the BD LSR Fortessa flow cytometer and FACSDiva 6.0 software. Data were analyzed using FlowJo software v10.

Animal models of Treg depletion and preterm birth in the first and second pregnancy

Partial depletion (25 μg/kg) or total depletion (50 μg/kg) of Tregs was performed in *Foxp3*^{DTR} dams as described above, and secondary injections (5 μg/kg or 50 μg/kg, respectively) were repeated every 24 h until delivery. Control dams were injected with 200 μL of sterile 1X PBS. Following injection, dams were monitored by infrared camera (Sony, Tokyo, Japan) until delivery. Gestational length was calculated from the presence of the vaginal plug until the appearance of the first pup in the cage bedding. Preterm birth was defined as delivery of all pups < 18.5 dpc. Neonatal survival and weights were recorded at birth and 1, 2, and 3 weeks postpartum. Photographs of neonates were also taken on the day of birth to verify breastfeeding. After 3 weeks of observation, dams were returned to mating cages to undergo a second pregnancy, underwent partial or total Treg depletion (or PBS injection) as described above, and were again monitored to determine pregnancy and neonatal outcomes until 3 weeks postpartum.

Fetal and placental weights from Treg-depleted dams

Foxp3^{DTR} dams were injected with 25 or 50 μg/kg of DT dissolved in 200 μL of sterile 1X PBS, or 200 μL of sterile 1X PBS alone, on 14.5 dpc. Twenty-four hours after injection, dams were injected with 5 or 50 μg/kg of DT dissolved in 200 μL of sterile 1X PBS, or 200 μL of sterile 1X PBS alone, respectively. Four hours later, dams were euthanized and the fetal and placental weights were measured using a scale (DIA-20; American Weights Scales, Norcross, GA, USA). Photographs of the fetuses and placentas were also taken.

Cell sorting and adoptive transfer of Tregs

Splenic Tregs were isolated from C57BL/6 dams at 10.5-13.5 dpc. Tregs were isolated using the mouse CD4+CD25+ Regulatory T Cell Isolation Kit, according to the manufacturer's instructions. The isolated Tregs were characterized (CD3+CD4+CD25+Foxp3+ cells) and quantified by flow cytometry prior to injection. *Foxp3*^{DTR} dams were injected intravenously with 1x10^{5} - 1x10^{6} Tregs/100 μL of sterile 1X PBS on 14.5 and 16.5 dpc. Two hours after the initial adoptive transfer, dams were i.p injected with 25 μg/kg of DT diluted in 200 μL of sterile 1X PBS. After 24 h, dams were injected with 5 μg/kg of DT diluted in 200 μL of sterile 1X PBS, which was repeated every 24 h until delivery. Following the second adoptive transfer, dams were monitored by infrared camera until delivery to record the rates of preterm birth and neonatal survival at birth. Neonatal survival was recorded at birth and 1, 2, and 3 weeks postpartum.

To determine the proportion of adoptively transferred Tregs present in peripheral and reproductive tissues, splenic Tregs were isolated from *EGFP* dams at 10.5-13.5 dpc. Tregs were isolated using the mouse CD4+CD25+ Regulatory T Cell Isolation Kit, according to the manufacturer's instructions. The isolated Tregs were characterized (CD3+CD4+CD25+Foxp3+ cells) and quantified by flow cytometry prior to injection. *Foxp3*^{DTR} dams were injected intravenously with 1x10^{5} - 1x10^{6} Tregs/100 μL of sterile 1X PBS on 14.5 and 16.5 dpc. Two hours after the initial adoptive transfer, dams were i.p injected with 25 μg/kg of DT diluted in 200 μL of sterile 1X PBS. After 24 h, dams were injected with 5 μg/kg of DT diluted in 200 μL of sterile 1X PBS, which was repeated until 17.5 dpc. On 18.5 dpc, dams were euthanized and the decidual, myometrial, and placental tissues were collected, as well as the peripheral blood and lymphatic tissues. Leukocyte isolation and immunophenotyping of Tregs was performed as described above to determine the proportion of adoptively transferred Tregs present in each tissue.

Measurement of maternal-fetal obstetrical parameters

Partial depletion (25 μg/kg) or total depletion (50 μg/kg) of Tregs was performed in *Foxp3*^{DTR} dams as described above, and secondary injections (5 μg/kg or 50 μg/kg, respectively) were repeated every 24 h until 17.5 dpc. Control dams were injected with 200 μL of sterile 1X PBS. On 17.5 dpc, three hours after injection, body temperature was evaluated using a rectal probe (TMH-150; VisualSonics Inc., Toronto, ON, Canada). Next, dams were placed in a restrainer and the arterial blood pressure was measured in the tail using a non-invasive method, according to manufacturer's instructions (Noninvasive Blood Pressure System, CODA High Throughput System; Kent Scientific Corporation, Torrington, CT, USA). The systolic, diastolic, and mean pressures were registered. Afterward, dams were anesthetized by inhalation of 2%–3% isoflurane (Aerrane; Baxter Healthcare Corporation, Deerfield, IL, USA) and 1-2 L/min of oxygen in an induction chamber. Anesthesia was maintained with a mixture of 1.75%–2% isoflurane and 2.0 L/min of oxygen during the ultrasound procedure, which was performed using the Vevo 2100 Imaging System (VisualSonics Inc.) as previously described (St Louis et al., 2016, Gomez-Lopez et al., 2016a, Arenas-Hernandez et al., 2019). Three fetuses from each dam were evaluated, including the first fetus in each uterine horn. The fetal and maternal heart rates and the pulsatility indices (PI) were examined in the right and left uterine arteries as well as in the umbilical artery using the 55-MHz linear ultrasound probe (VisualSonics Inc.). The PI was calculated using the following formula: [PI = (peak systolic velocity – end diastolic velocity)/mean velocity]. Ultrasound signals were processed, displayed, and stored using the Vevo Imaging Station (VisualSonics Inc.). Following the ultrasound procedure, dams were euthanized and photographs of the maternal spleen and ULN were taken.

Model of susceptibility to endotoxin-induced preterm birth after Treg depletion

Foxp3^{DTR} dams were injected i.p. with an initial dose of 25 μg/kg of DT diluted in 200 μL of sterile 1X PBS on 14.5dpc. Twenty-four hours post-injection, dams received a second injection of 25 μg/kg of DT diluted in 200 μL of sterile 1X PBS. On 16.5 dpc, *Foxp3*^{DTR} dams were injected with 2 μg/200 μL of lipopolysaccharide (LPS) from *Escherichia coli* (O55:B5; Sigma-Aldrich). Non-Treg-depleted control *Foxp3*^{DTR} dams were injected with sterile 1X PBS on 14.5 and 15.5 dpc and 2 μg/200 μL of LPS on 16.5 dpc. Controls also included *Foxp3*^{DTR} dams injected with DT only on 14.5 and 15.5 dpc. Following injection, dams were monitored by infrared camera until delivery to record the rates of preterm birth. Neonatal survival was recorded at birth and 1, 2, and 3 weeks postpartum.

Determination of cytokine concentrations in the maternal circulation and amniotic fluid

Foxp3^{DTR} dams were injected with 25 or 50 μg/kg of DT dissolved in 200 μL of sterile 1X PBS, or 200 μL of sterile 1X PBS alone, on 14.5dpc. Twenty-four hours after injection, dams were injected with 5 or 50 μg/kg of DT, respectively, dissolved in 200 μL of sterile 1X PBS, or 200 μL of sterile 1X PBS alone. Four hours later, dams were euthanized and peripheral blood was collected by cardiac puncture for plasma separation. Amniotic fluid was also obtained from each amniotic sac with a 26-gauge needle. To determine the cytokine storm in endotoxin-induced preterm birth, C57BL/6 dams were i.p. injected with 10 μg of LPS dissolved in 200 μL of sterile 1X PBS on 16.5 dpc. Dams were euthanized on 17.5 dpc and peripheral blood was collected by cardiac puncture for plasma separation. Maternal plasma and amniotic fluid samples were centrifuged at 800 or 1300 x g, respectively, for 10 min at 4°C and the supernatants were separated and stored at −20°C until analysis. The ProcartaPlex Mouse Cytokine & Chemokine Panel 1A 36-plex (Invitrogen by Thermo Fisher Scientific, Vienna, Austria) was used to measure the concentrations of IFNγ, IFNα, IL-12p70, IL-1β, TNFα, GM-CSF, IL-18, IL-17A, IL-22, IL-23, IL-27, IL-9, IL-15/IL-15R, IL-13, IL-2, IL-4, IL-5, IL-6, IL-10, CCL11, IL-28, IL-3, LIF, IL-1α, IL-31, CXCL1, CCL3, CXCL10, CCL2, CCL7, CCL4, CXCL2, CCL5, G-CSF, M-CSF, and CXCL5 in maternal plasma and amniotic fluid samples, according to the manufacturer's instructions. Plates were read using the FLEXMAP 3D (Luminex Corporation, Austin, TX, USA), and analyte concentrations were calculated with ProcartaPlex Analyst 1.0 Software from Affymetrix, San Diego, CA, USA. The sensitiv-

ities of the assays were: 0.09 pg/mL (IFNγ), 3.03 pg/mL (IFNα), 0.21 pg/mL (IL-12p70), 0.14 pg/mL (IL-1β), 0.39 pg/mL (TNFα), 0.19 pg/mL (GM-CSF), 9.95 pg/mL (IL-18), 0.08 pg/mL (IL-17A), 0.24 pg/mL (IL-22), 2.21 pg/mL (IL-23), 0.34 pg/mL (IL-27), 0.28 pg/mL (IL-9), 0.42 pg/mL (IL-15/IL-15R), 0.16 pg/mL (IL-13), 0.10 pg/mL (IL-2), 0.03 pg/mL (IL-4), 0.32 pg/mL (IL-5), 0.21 pg/mL (IL-6), 0.69 pg/mL (IL-10), 0.01 pg/mL (CCL11), 20.31 pg/mL (IL-28), 0.11 pg/mL (IL-3), 0.28 pg/mL (LIF), 0.32 pg/mL (IL-1α), 0.45 pg/mL (IL-31), 0.05 pg/mL (CXCL1), 0.13 pg/mL (CCL3), 0.26 pg/mL (CXCL10), 3.43 pg/mL (CCL2), 0.15 pg/mL (CCL7), 1.16 pg/mL (CCL4), 0.37 pg/mL (CXCL2), 0.35 pg/mL (CCL5), 0.19 pg/mL (G-CSF), 0.02 pg/mL (M-CSF), and 5.67 pg/mL (CXCL5). Inter-assay and intra-assay coefficients of variation were less than 10%. Amniotic fluid cytokine concentrations were adjusted by protein concentration, which were determined using the Pierce BCA Protein Assay Kit (Pierce Biotechnology, Rockford, IL, USA), following the manufacturer's instructions.

Systemic injection of cytokines/chemokines in pregnant mice

C57BL/6 dams were intravenously injected with 1.4 pg of recombinant mouse IFNγ (Peprotech, Rocky Hill, NJ, USA), 218 pg of recombinant mouse CCL7 (R&D Systems, Minneapolis, MN, USA), or 48 pg of recombinant mouse IL-22 (Biolegend, San Diego, CA, USA), or a combination of these three cytokines, dissolved in 100 μL of sterile 1X PBS using a 26-gauge needle on 15.5, 16.5, and 17.5 dpc. Controls were injected with 100μL of sterile 1X PBS alone. Following injection, dams were monitored by infrared camera until delivery to record the rates of full or early term birth and neonatal mortality at birth, and neonates were monitored for up to 3 weeks after delivery.

Immunophenotyping of leukocytes from the decidual, myometrial, and placental tissues and peripheral blood

Foxp3^{DTR} dams were injected with 25 or 50 μg/kg of DT dissolved in 200 μL of sterile 1X PBS, or 200 μL of sterile 1X PBS alone, on 14.5dpc. Twenty-four hours after injection, dams were injected with 5 or 50 μg/kg of DT, respectively, dissolved in 200 μL of sterile 1X PBS, or 200 μL of sterile 1X PBS alone. Four hours later, dams were euthanized and the decidual, myometrial, and placental tissues, as well as the peripheral blood, were collected. The PBMCs were isolated from peripheral blood by density gradient using Ficoll-Paque Plus and washed with 1X PBS. Leukocyte suspensions were prepared from decidual, myometrial, and placental tissues as previously described (Arenas-Hernandez et al., 2015), and were stained using the BD Fixable Viability Stain 510 prior to incubation with anti-mouse mAbs (Key Resources Table). Leukocyte suspensions were centrifuged at 1,250 x g for 10 min at 4°C in the dark. Cells were then incubated with the CD16/CD32 mAb (FcγIII/II receptor) for 10 min and subsequently incubated with specific fluorochrome conjugated anti-mouse mAbs (Key Resources Table) for 30 min at 4°C in the dark. Leukocyte suspensions were fixed/permeabilized with the BD Cytofix/Cytoperm Fixation/Permeabilization Kit or Foxp3/Transcription Factor Staining Buffer Set prior to straining with intracellular or intranuclear anti-mouse mAbs. Cells were acquired using the BD LSR Fortessa flow cytometer and FACSDiva 6.0 software. Immunophenotyping included the identification of macrophages (CD45+CD11b+F4/80+Ly6G- cells), neutrophils (CD45+CD11b+F4/80-Ly6G+ cells), dendritic cells (DCs; CD45+CD11b+F4/80-CD11c+CD205+ cells), NK cells (CD45+CD11b-CD49b+ cells), T cells (CD3+ cells), CD4+ T cells (CD3+CD4+ cells), CD8+ T cells (CD3+CD8+ cells), and B cells (CD45+CD11b-CD19+ cells) in the decidual, myometrial, and placental tissues as well as in the maternal circulation. The activation status of these cells was determined by cytokine expression (Key Resources Table). Data were analyzed using FlowJo software v10. Log2 fold changes in cell abundance (frequencies) were determined and represented in heatmaps.

RNA-seq analysis of placental tissues

RNA isolation, library preparation, and sequencing: Partial depletion (25 μg/kg) or total depletion (50 μg/kg) of Tregs was performed in *Foxp3*^{DTR} dams on 14.5 dpc as described above, and secondary injections (5 μg/kg or 50 μg/kg, respectively) were performed 24 h after (15.5 dpc). Four hours later, dams were euthanized and the placental tissues were collected from implantation sites and placed in RNA*later* Stabilization Solution (Life Technologies). Total RNA was isolated from tissues using the RNeasy mini kit (QIAGEN, Hilden, Germany), following the manufacturer's instructions. RNA concentrations and purity were assessed with the NanoDrop 1000 spectrophotometer (Thermo Fisher Scientific), and RNA integrity was evaluated with the 2100 Bioanalyzer system (Agilent Technologies, Wilmington, DE) using the Agilent RNA 6000 Nano Kit (Agilent Technologies). The RNA-Seq library was prepared by the Beijing Genomics Institute (BGI; Wuhan, China) using the MGIEasy RNA Library Prep kit (MGI Americas Inc., San Jose, CA, USA). Paired-end reads of 150 bp length were sequenced on the BGISEQ-500RS sequencer (BGI), and raw data were provided by BGI.

Pre-processing of RNA-Seq data: Paired-end RNA-Seq sequence data in *fastq* format were processed using Salmon aligner v0.12.0 (Patro et al., 2017) in quasi-mapping mode using a transcriptome index prepared from *Mus musculus* genome assembly *GRCm38* (mm10). Transcripts per million (TPM) values from Salmon output were scaled up to library size and imported into R (version 3.5.2) using the *tximport* package of Bioconductor (Gentleman et al., 2004, Soneson et al., 2015).

Assessment of differences between treatment groups: Count data were analyzed using negative binomial models implemented in the *DESeq2* package (Anders et al., 2013). Only genes that had counts > 5 in at least five samples were retained for further analysis. Genes were considered to be differentially expressed if the fold change between groups was > 1.25 and the false discovery rate (Benjamini and Hochberg, 1995) adjusted p value was < 0.1.

RNA-Seq data visualization: The RNA-Seq data (log2 counts) for the top 50 upregulated and top 50 downregulated genes were visualized using heatmaps with hierarchical clustering of genes.

Biological process determination: Over-representation of biological processes among significantly up- and down- regulated genes was determined separately by performing hypergeometric tests using the stringApp v1.5.0 (Doncheva et al., 2019) in Cytoscape v3.7.2 (Otasek et al., 2019). The stringApp was also used to visualize known interactions between proteins coded by the differentially expressed genes in selected biological processes. Over-representation of biological processes among all differentially expressed genes, regardless of their direction of change, was also tested with ClueGO v2.5.5 (Mlecnik et al., 2019) and the significantly disrupted biological processes were grouped based on their functional annotation and visualized as a network of gene ontologies. A q-value cutoff of < 0.05 was used to determine significance of enrichment analysis.

QUANTIFICATION AND STATISTICAL ANALYSIS

Statistical Analysis

Statistical analyses were performed using SPSS v19.0 (IBM, Armonk, NY, USA) or the R package (version 3.5.2). For human demographic data, the group comparisons were performed using the Fisher's test with Monte-Carlo simulation for proportions and Kruskal-Wallis tests for non-normally distributed continuous variables. The Mann-Whitney U-test was used to compare differences between the groups for human flow cytometry data. The Fisher's exact test was used to compare the rates of preterm birth. The Kaplan-Meier survival curves were used to plot and compare the neonatal survival data (Mantel-Cox test). The Kruskal-Wallis and ANOVA tests were utilized for comparisons among groups for murine observational and obstetrical data as well as for maternal plasma and amniotic fluid cytokine concentrations. A p value ≤ 0.05 was considered statistically significant. For flow cytometry heatmaps, the statistical significance of differences between study groups were assessed using t tests followed by the false discovery rate adjustment of p values, with a $q < 0.1$ being considered significant (represented as asterisks in the heatmap). RNA-Seq analysis was performed as described above.

Cell Reports, Volume *32*

Supplemental Information

Regulatory T Cells Play a Role in a Subset of Idiopathic Preterm Labor/Birth and Adverse Neonatal Outcomes

Nardhy Gomez-Lopez, Marcia Arenas-Hernandez, Roberto Romero, Derek Miller, Valeria Garcia-Flores, Yaozhu Leng, Yi Xu, Jose Galaz, Sonia S. Hassan, Chaur-Dong Hsu, Harley Tse, Carmen Sanchez-Torres, Bogdan Done, and Adi L. Tarca

Table S1. Clinical and demographic characteristics of the human study groups utilized for suppressive assays, related to Figure 1.

Clinical characteristics	Preterm (n = 6)	Term (n = 8)	p-value
Maternal age (years; median [IQR])[a]	28.5 (22.3-34.8)	27.5 (25.3-33.3)	0.7
Body mass index (kg/m^2; median [IQR])[a]	33.1 (30.8-42.5)	27 (24.3-31.9)	0.1
Primiparity[b]	16.7% (1/6)	12.5% (1/8)	1
Race/Ethnicity[b]			0.4
Black	83.3% (5/6)	100% (8/8)	
White	16.7% (1/6)	0% (0/8)	
Gestational age at delivery (weeks; median [IQR])[a]	35.5 (34.5-35.9)	40.1 (39.7-40.6)	0.002
Cesarean section[b]	50% (3/6)	37.5% (3/8)	1
Birthweight (grams; median [IQR])[a]	2122.5 (1773.8-2201.3)	3205 (3058.8-3551.3)	0.002

Data are given as median (interquartile range, IQR) and percentage (n/N).
[a]Mann-Whitney U test.
[b]Fisher's exact test

Table S2. Clinical and demographic characteristics of the human study groups utilized for flow cytometry studies, related to Figure 1 and Figure 2.

Clinical characteristics	PTNL (n = 28)	iPTL (n = 19)	iPTL+CI (n = 21)	PTL+AI (n = 13)	TNL (n = 13)	TIL (n = 13)	TIL+CI (n = 19)	TIL+AI (n = 14)	p-value
Maternal age (years; median [IQR])[a]	25 (22-31.8)	23 (20-29)	25 (23-30)	23 (21-25)	27 (25-28)	24 (22-28)	25 (21-33)	23 (21.5-29)	0.2
Body mass index (kg/m^2; median [IQR])[a]	27.9 (24.9-37.6)[c]	25.4 (23.5-32.8)[c]	24.9 (21.8-32.4)[c]	25.8 (24.1-28.3)[c]	28.9 (25-30.4)	25.7 (23.7-31.5)[c]	28.2 (23.8-34.2)	31 (23.6-39.8)	0.7
Primiparity[b]	21.4% (6/28)	31.6% (6/19)	9.5% (2/21)	15.4% (2/13)	15.4% (2/13)	23.1% (3/13)	26.3% (5/19)	28.6% (4/14)	0.7
Race/Ethnicity[b]									0.06
Black	82.1% (23/28)	79% (15/19)	81% (17/21)	92.3% (12/13)	61.5% (8/13)	92.3% (12/13)	94.7% (18/19)	100% (14/14)	
White	14.3% (4/28)	10.5% (2/19)	4.8% (1/21)	0% (0/13)	23.1% (3/13)	7.7% (1/13)	0% (0/19)	0% (0/14)	
Asian	0% (0/28)	10.5% (2/19)	0% (0/21)	0% (0/13)	15.4% (2/13)	0% (0/13)	0% (0/19)	0% (0/14)	
Hispanic	0% (0/28)	0% (0/19)	0% (0/21)	7.7% (1/13)	0% (0/13)	0% (0/13)	0% (0/19)	0% (0/14)	
Other	3.6% (1/28)	0% (0/19)	14.3% (3/21)	0% (0/13)	0% (0/13)	0% (0/13)	5.3% (1/19)	0% (0/14)	
Gestational age at delivery (weeks; median [IQR])[a]	32.4 (28.9-34.7)	35.1 (34.2-36.2)	35.1 (31.9-36.4)	29.3 (22-31.9)	39.1 (39-39.3)	39 (38.6-40.3)	39.1 (38.2-40)	40.7 (39.1-41.1)	<0.001
Cesarean section[b]	100% (28/28)	31.6% (6/19)	9.5% (2/21)	15.4% (2/13)	100% (13/13)	15.4% (2/13)	10.5% (2/19)	21.4% (3/14)	<0.001
Birthweight (grams; median [IQR])[a]	1522.5 (951.8-2202.5)	2395 (2205-2700)	2020 (1755-2355)	1290 (399-1665)	3085 (2915-3615)	3040 (2865-3240)	3170 (2880-3552.5)	3422.5 (3037.5-3670)	<0.001
Maternal inflammatory response (moderate/severe acute chorioamnionitis)[b]	0% (0/28)	0% (0/19)	0% (0/21)	100% (13/13)	0% (0/13)	0% (0/13)	0% (0/19)	100% (14/14)	<0.001
Fetal inflammatory response (moderate/severe acute funisitis)[b]	0% (0/28)	0% (0/19)	0% (0/21)	53.9% (7/13)	0% (0/13)	0% (0/13)	0% (0/19)	14.3% (2/14)	<0.001

Data are given as median (interquartile range, IQR) and percentage (n/N). PTNL = preterm without labor; iPTL = idiopathic preterm labor; PTL+AI = preterm labor associated with intra-amniotic inflammation/infection; TNL = term without labor; TIL = term with labor; CI = chronic inflammatory lesions of the placenta; AI = acute inflammatory lesions of the placenta.

[a]Kruskal-Wallis test.

[b]Fisher's test with Monte-Carlo simulation.

[c]Some missing data

A

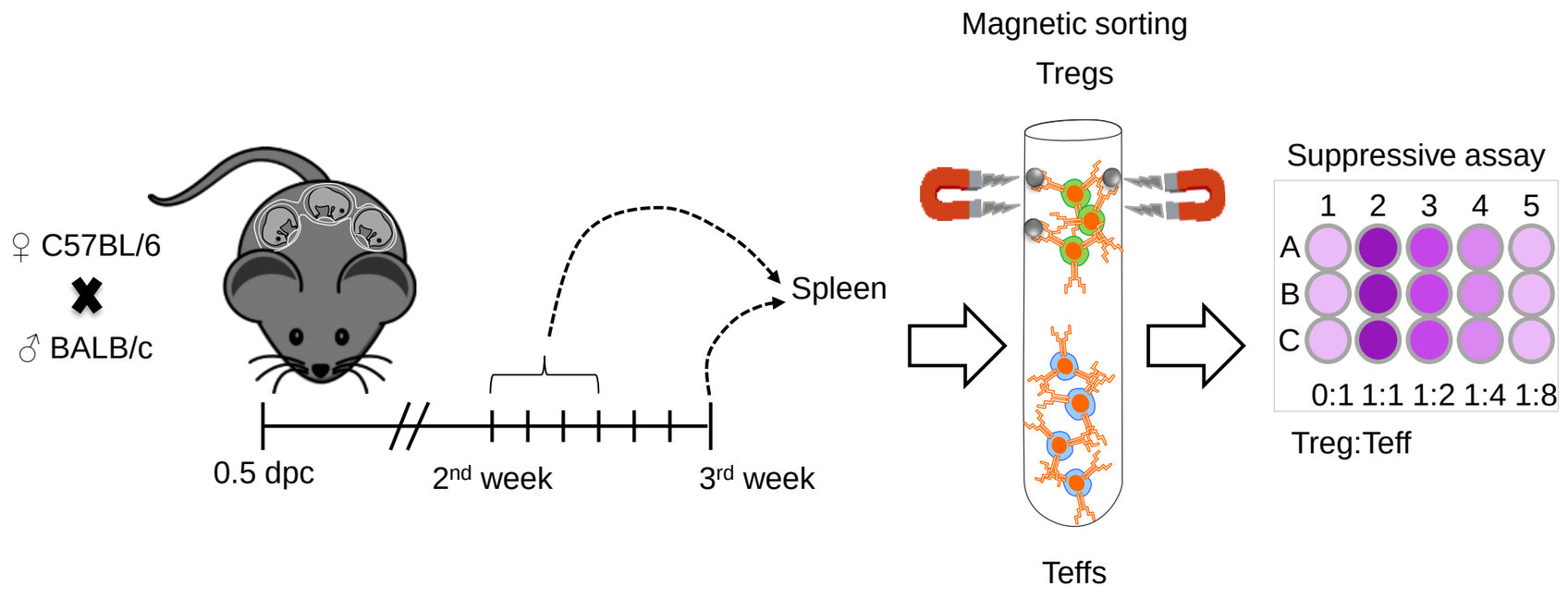

B

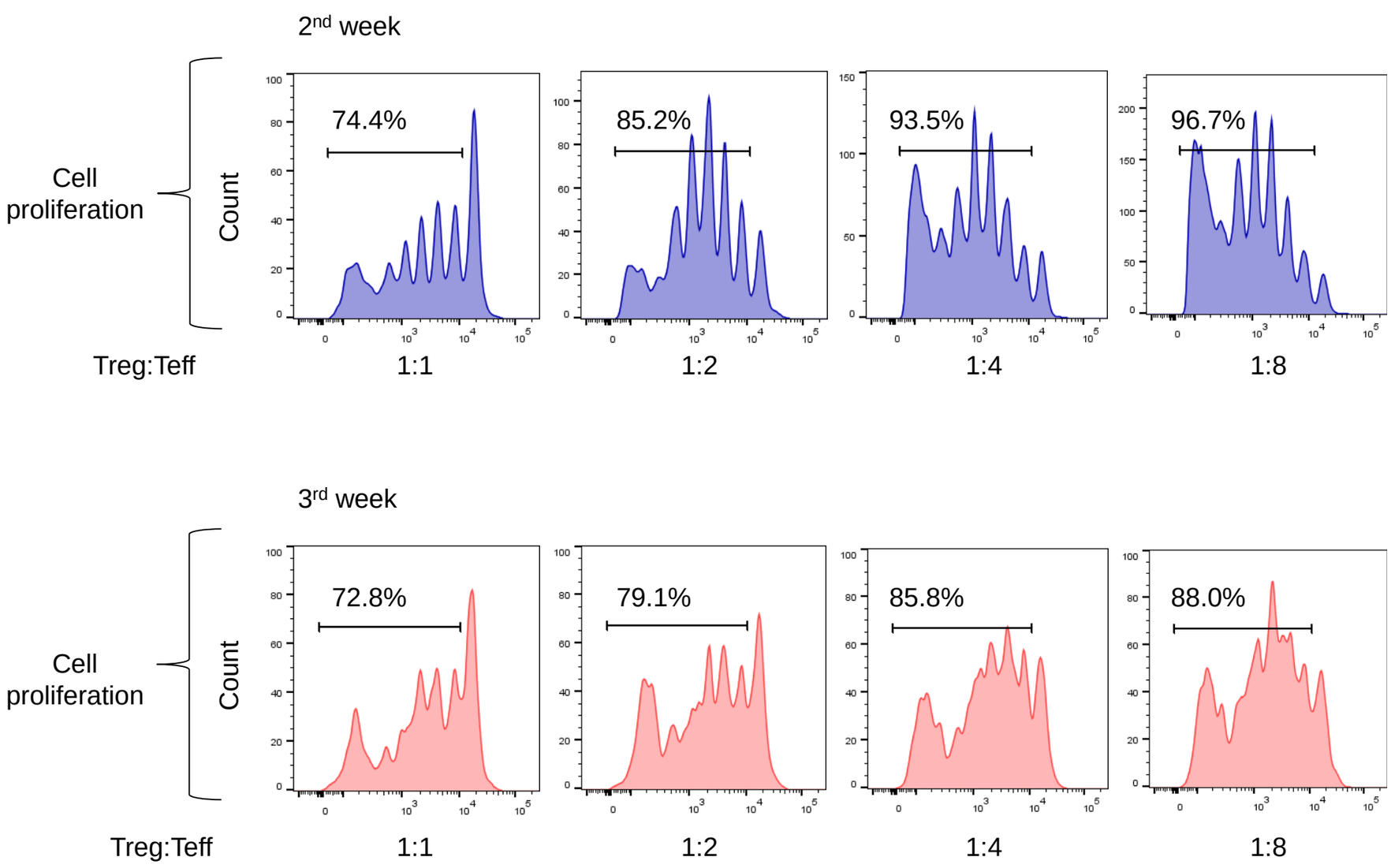

C

D

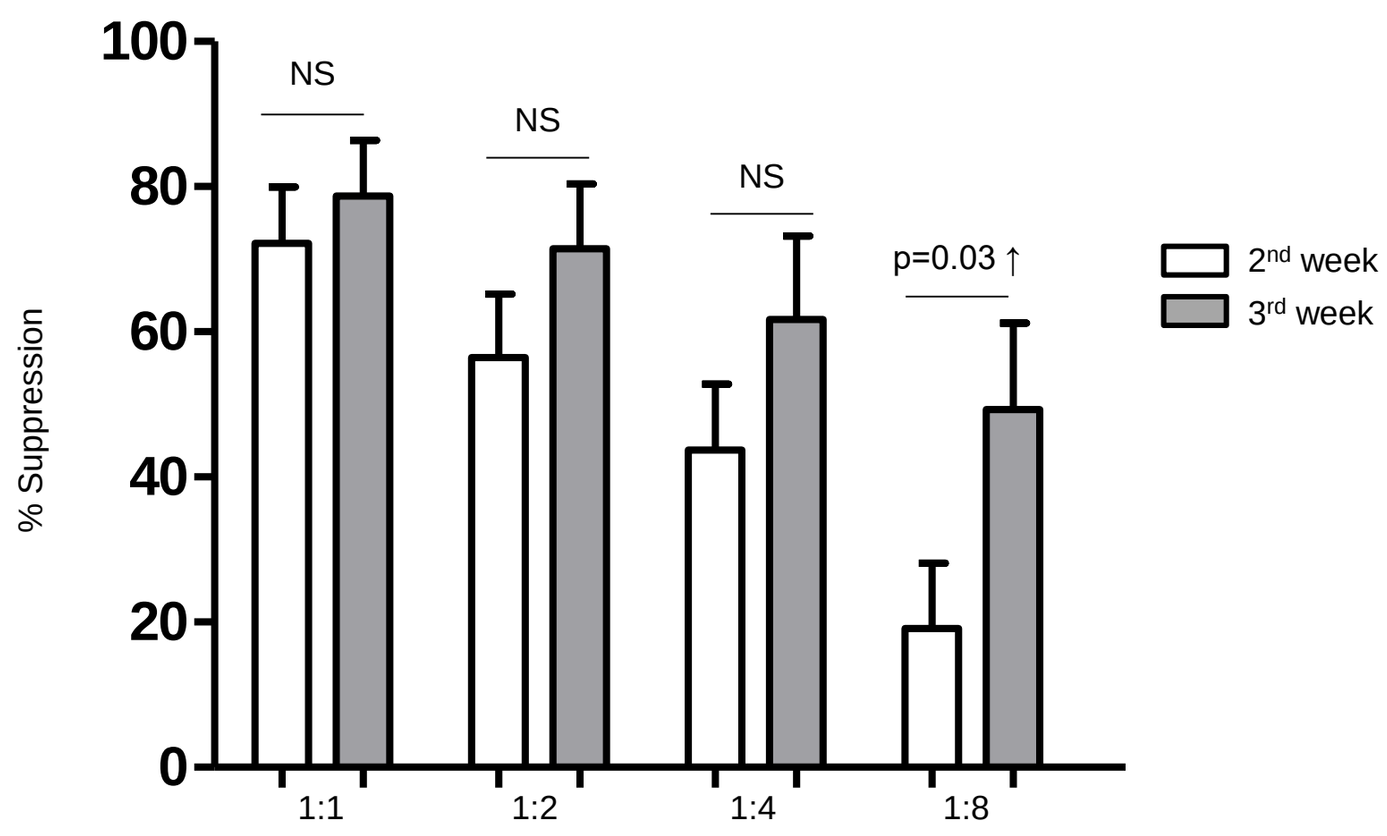

Figure S1. Suppressive function of murine regulatory T cells during the 2nd or 3rd week of pregnancy, related to Figure 3. (A) The spleen was collected from C57BL/6 dams in the 2nd or 3rd week of pregnancy for the magnetic isolation of splenic regulatory T cells (Tregs) and effector T cells (Teffs or Teff cells). Tregs were co-cultured with Teff cells at a 0:1, 1:1, 1:2, 1:4, or 1:8 Treg:Teff ratio for 96 h and Teff cell proliferation was measured by flow cytometry using CellTrace Violet. **(B)** Representative plots showing the proliferation of Teff cells in the 2nd week of pregnancy. **(C)** Representative plots showing the proliferation of Teff cells in the 3rd week of pregnancy. **(D)** Percentage of splenic Treg suppression of Teff cells in the 2nd or 3rd week of pregnancy (n = 4-6 per group). Data are shown as means ± SEM. Statistical analysis was performed using Mann-Whitney U tests.

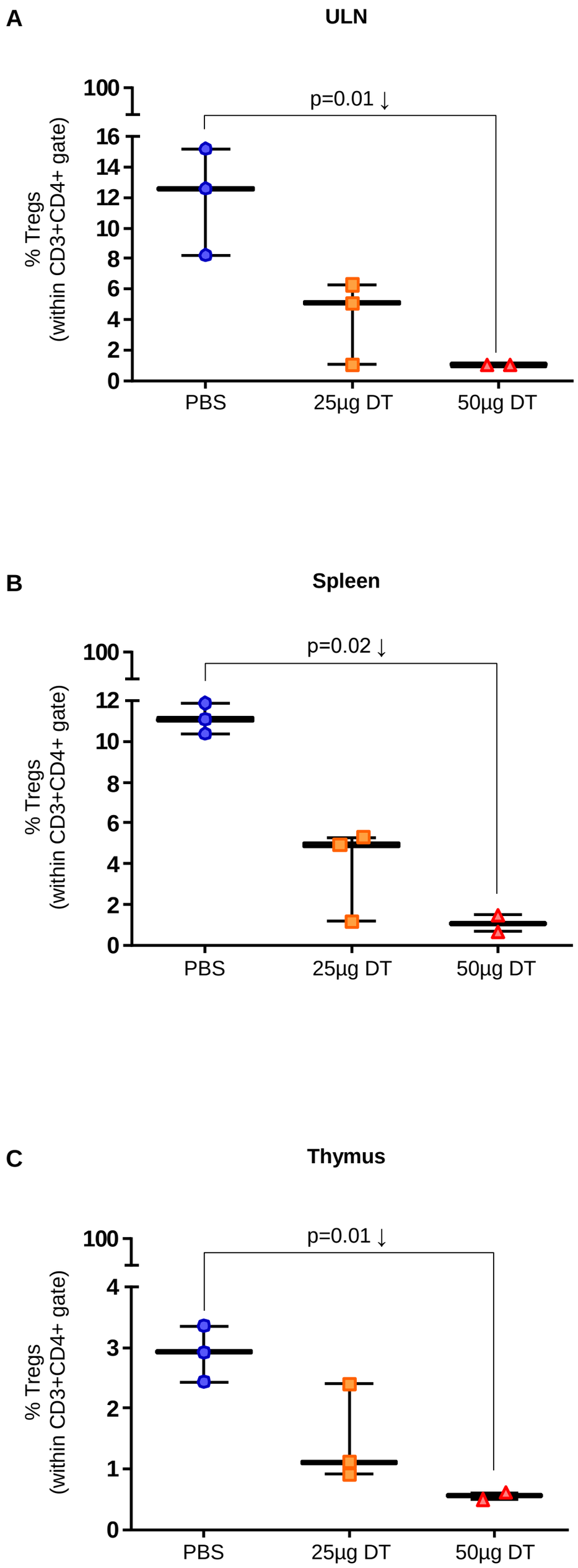

Figure S2. Depletion of regulatory T cells in non-pregnant *Foxp3*^{DTR} mice, related to Figure 3. *Foxp3*^{DTR} naïve females underwent partial or total regulatory T cell (Treg) depletion. Controls were injected with sterile 1X PBS. Mice were euthanized approximately 4 h after the second DT or PBS injection and tissues were collected for determination of Tregs. The frequencies of Tregs in the **(A)** uterine-draining lymph nodes (ULN), **(B)** spleen, and **(C)** thymus of non-Treg-depleted-, partially Treg-depleted-, and totally Treg-depleted-*Foxp3*^{DTR} mice (n = 2-3 per group). Data are shown as medians with minimum/maximum ranges. Statistical analysis was performed using Kruskal-Wallis tests with correction for multiple comparisons.

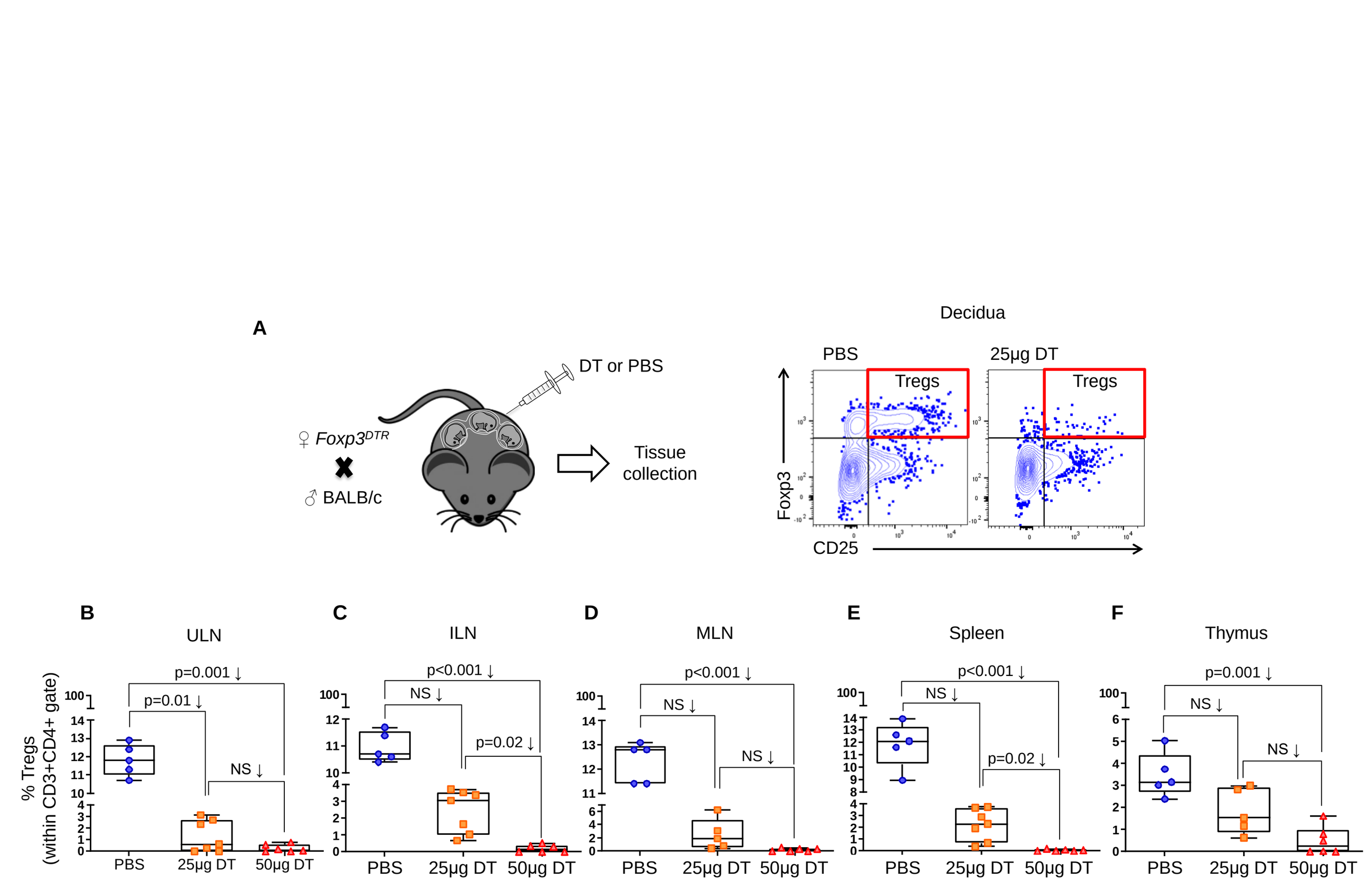

Figure S3. Depletion of regulatory T cells in pregnant *Foxp3^{DTR}* mice, related to Figure 3. (A) *Foxp3^{DTR}* dams underwent partial or total regulatory T cell (Treg) depletion. Controls were injected with sterile 1X PBS. Mice were euthanized approximately 4 h after the second DT or PBS injection and tissues were collected for determination of Tregs. Representative gating strategy of Treg depletion in the decidua is shown. The frequencies of Tregs in the **(B)** uterine-draining lymph nodes (ULN), **(C)** inguinal lymph nodes (ILN), **(D)** mesenteric lymph nodes (MLN), **(E)** spleen, and **(F)** thymus of non-Treg-depleted-, partially Treg-depleted-, and totally Treg-depleted-*Foxp3^{DTR}* dams (n = 5-7 per group). Data are shown as medians with interquartile ranges and minimum/maximum ranges. Statistical analysis was performed using Kruskal-Wallis tests with correction for multiple comparisons.

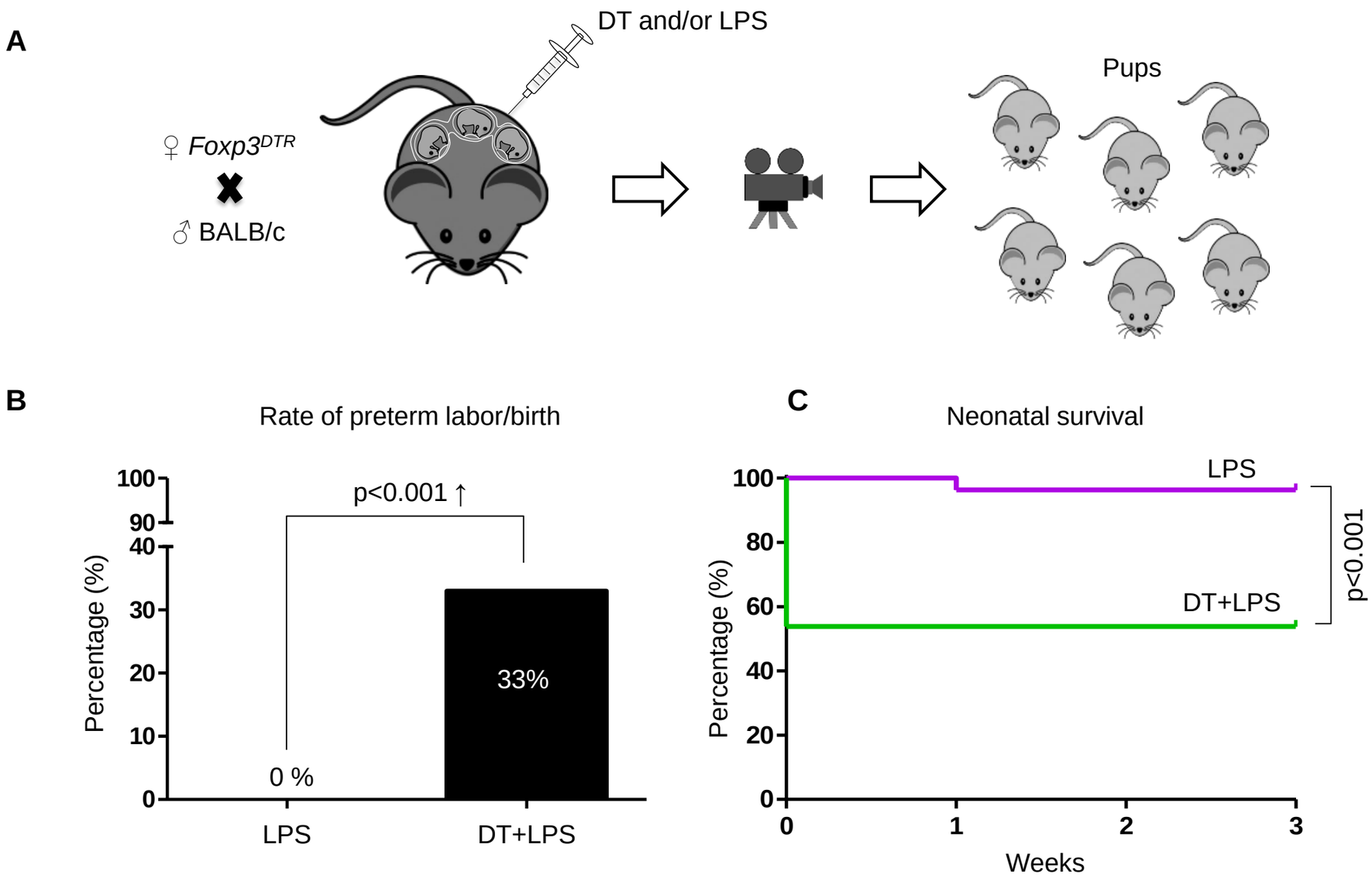

Figure S4. Depletion of Tregs increases the susceptibility to endotoxin-induced preterm birth, related to Figure 3. (A) *Foxp3*^{DTR} dams underwent partial regulatory T cell (Treg) depletion. On 16.5 dpc, a single intraperitoneal injection of 2 μg/200 μL of lipopolysaccharide (LPS; endotoxin) was given. Controls also included *Foxp3*^{DTR} dams injected with DT only on 14.5 and 15.5 dpc (data not shown). **(B)** Preterm birth rates of non-Treg-depleted- or partially Treg-depleted-*Foxp3*^{DTR} dams injected with LPS (n = 9 per group). Data are represented as means. **(C)** Percentage of survival from birth until 3 weeks postpartum for neonates born to non-Treg-depleted- or partially Treg-depleted- *Foxp3*^{DTR} dams injected with LPS (n = 5-8 per group). Statistical analyses were performed using the Fisher's exact test for rate of preterm birth or Mantel-Cox test for survival curves.

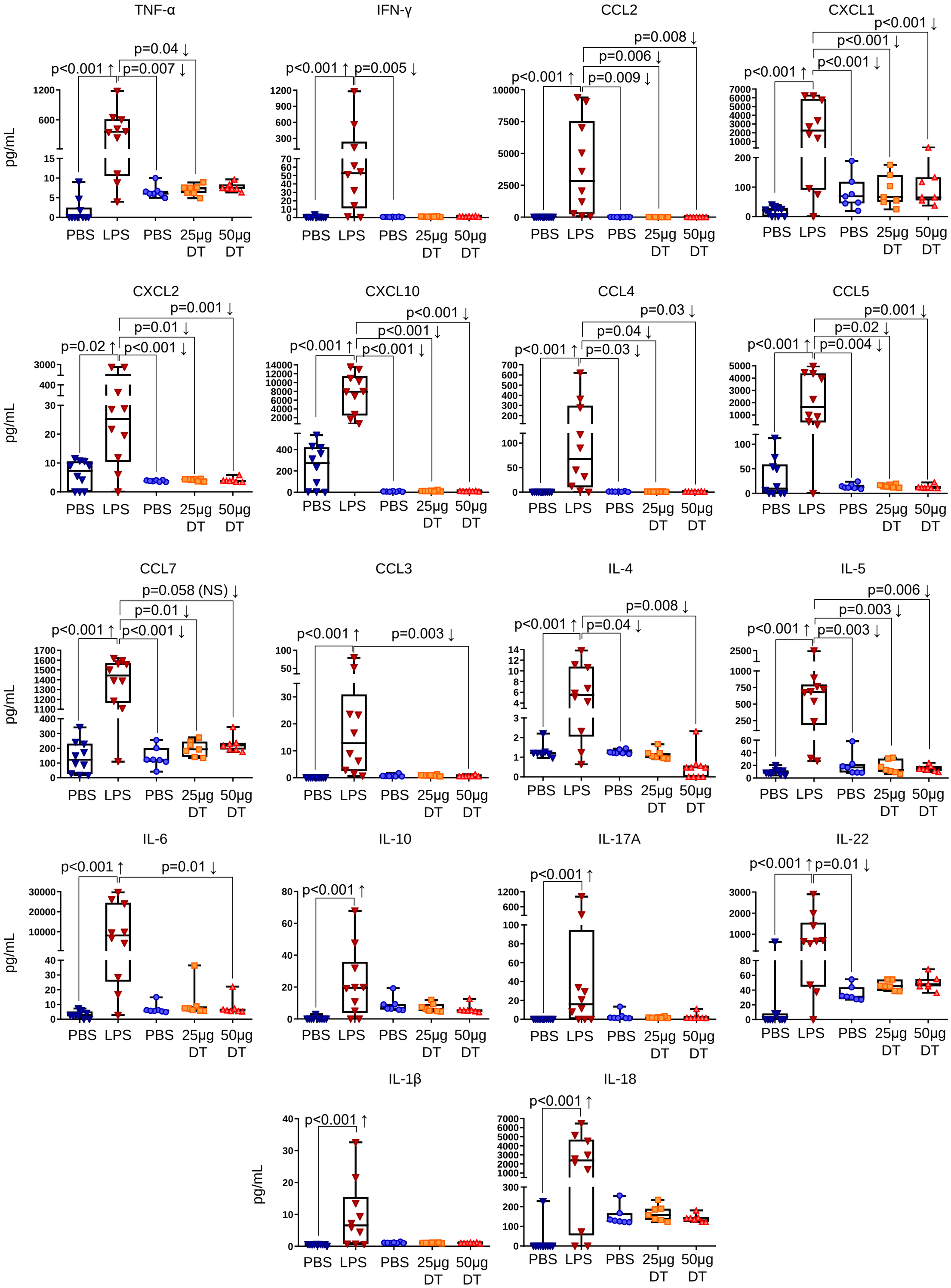

Figure S5. Comparison of the systemic acute proinflammatory response in the endotoxin-induced preterm birth model and the Treg-depletion induced preterm birth model, related to Figure 6. C57BL/6 dams were intraperitoneally injected with 10 μg/200 μL of lipopolysaccharide (LPS; endotoxin) or sterile 1X PBS on 16.5 dpc. Mice were euthanized on 17.5 dpc and maternal plasma was collected for cytokine and chemokine determination (n = 10 per group). *Foxp3*^{DTR} dams underwent partial or total regulatory T cell (Treg) depletion. Non-Treg-depleted controls were injected with sterile 1X PBS. Mice were euthanized approximately 4 h after the second injection and maternal plasma was collected for cytokine and chemokine determination (n = 7 per group). Data are shown as medians with interquartile ranges and minimum/maximum ranges. Statistical analysis was performed using Kruskal-Wallis or ANOVA tests with correction for multiple comparisons.

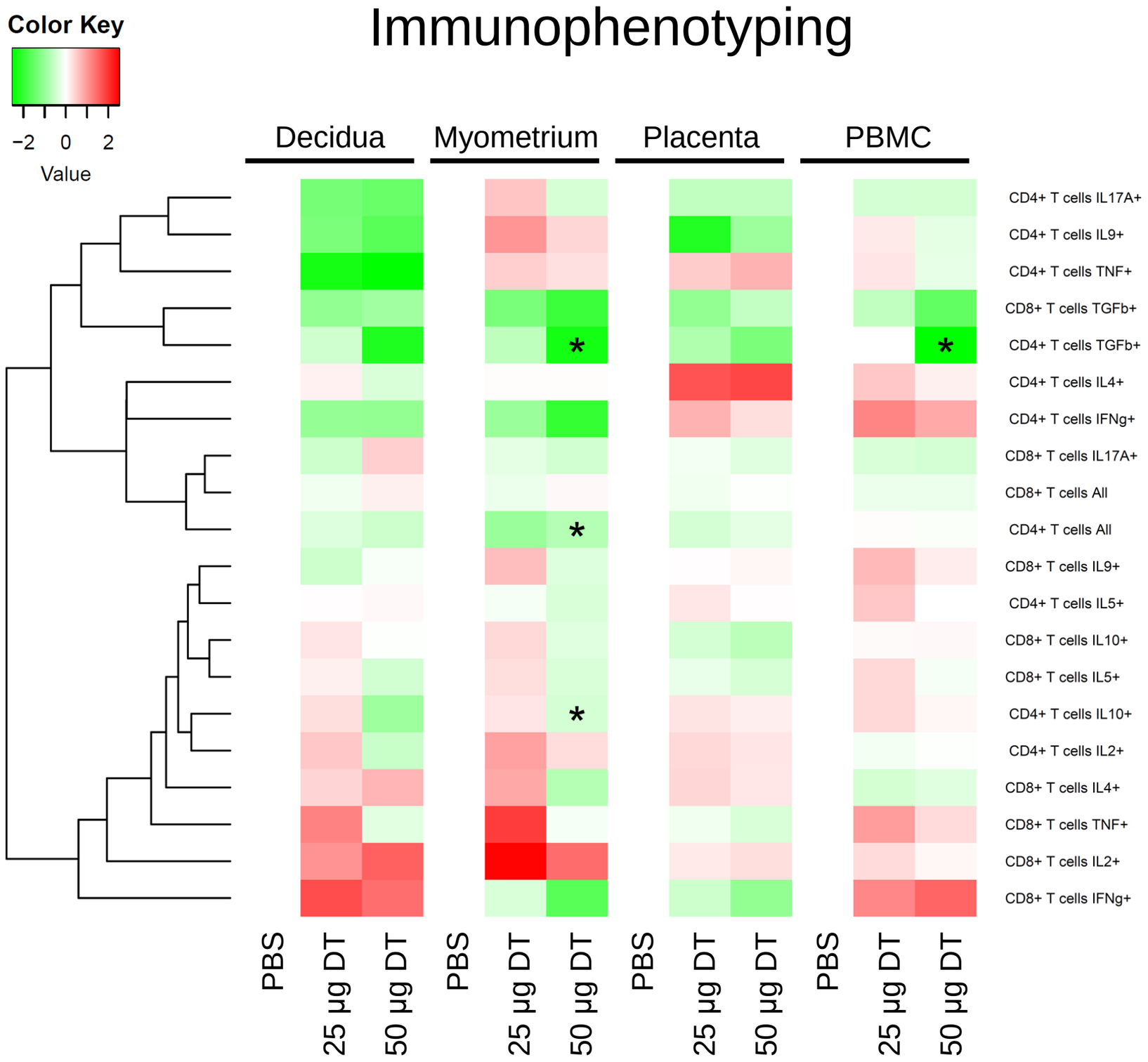

Figure S6. Depletion of Tregs is associated with altered local and systemic T-cell responses, related to Figure 7. Foxp3^{DTR} dams underwent partial or total regulatory T cell (Treg) depletion. Controls were injected with sterile 1X PBS. Mice were euthanized approximately 4 h after the second injection and the decidua, myometrium, placenta, and peripheral blood were collected for immunophenotyping (n = 5-7 per group). Heatmap visualization of changes in the frequencies of T-cell subsets in the decidua, myometrium, placenta, and peripheral blood of partially and totally Treg-depleted Foxp3^{DTR} dams relative to non-Treg-depleted controls. Red indicates increased frequency and green indicates decreased frequency. Statistical analysis was performed using t-tests with false discovery rate adjustment. Asterisks indicate significant differences compared to controls after adjustment.